Flood Control 2015

Relation between accuracy of floodplain roughness parameterization and uncertainty in 2D hydrodynamic models

Menno Straatsma, Fredrik Huthoff

ITC UNIVERSITY OF TWENTE.
FACULTY OF GEO-INFORMATION SCIENCE AND EARTH OBSERVATION

HKV CONSULTANTS

Relation between accuracy of floodplain roughness parameterization and uncertainty in 2D hydrodynamic models

Corresponding author: Menno Straatsma
Email: straatsma@itc.nl
Status: final

Table of contents

List of figures

List of tables

Abstract

Introduction
Flood risk has significantly increased over the last four decades, quantified as the number of reported occurrences and the number of people affected. Hydrodynamic models are used routinely within the framework of disaster risk management to compute flood risk and reduce economic damage and human suffering. They are used to model inundation extent, water depth and flow velocity for flood hazard assessment. While a lot of progress has been made in solving the flow equations efficiently and reliably uncertainty reduction has remained a major issue. The current study aims at providing better insight into the uncertainty of flood water levels due to uncertain floodplain roughness parameterization. The study focuses on three key elements in the uncertainty of floodplain roughness: (1) classification error of the land cover map, (2), within class variation of vegetation structural characteristics, and (3) mapping scale.

Methods
To assess the effect of the first error source, new realizations of ecotope maps were made based on the current floodplain ecotope map and an error matrix of the classification. Uncertainty in classification of the terrestrial ecotopes of the Rhine branches has been determined as “map purities”, referring to the percentage of the mapped area that is correctly classified. A few problems were noted with the fieldwork related to the discernability of the different ecotopes in the field. Also, the spatial support of the field data (point measurements) did not match the aerial image interpretation of ecotopes per polygon, sized 400 m^2 or more. Therefore the reported classification accuracy should be interpreted as a minimum value. Fifteen model runs were carried out with a classification accuracy of 69, 80, 90, and 95 percent to determine the effect of classification accuracy on uncertainty in the peak water levels. For within class variation, few data were available. Therefore, field measurements of vegetation structure were compiled to obtain uncertainty ranges for each vegetation structural type. The scale error was investigated by reassigning roughness codes on a smaller spatial scale.

Results and conclusion
It is shown that the various error-sources lead to large variation in floodplain roughness. Classification error proved to be the largest contributor to the uncertainty. Even at the 95 % classification accuracy, the variation in peak water levels was higher than for the vegetation structural error and the scale error. The associated uncertainty of predicted water levels is in the order of decimeters for classification error and cm for within class variation and scale errors. The relation between uncertain floodplain roughness and the error bands in water levels may serve as a guideline for the desired accuracy of floodplain characteristics in hydrodynamic models. However, these should not be interpreted as absolute uncertainty bands as no calibration has been applied. Therefore the next step will be to determine the absolute uncertainty when the models are calibrated and make the link to operational flood forecasting.

1. Introduction

Uncertainty reduction in operational flood forecasting has been a major topic over the last years to accurately predict flood levels for alluvial areas. Hydrodynamic models are used routinely within this framework. They are used to model inundation extent, water depth and flow velocity for flood hazard assessment. While a lot of progress has been made in solving the flow equations efficiently and reliably (Hunter et al., 2007; Bates et al., 2010) uncertainty reduction has remained a major issue., especially in the field of operational flood forecasting.

Walker et al. (2003) defined uncertainty as "any departure from the unachievable ideal of complete determinism." Uncertainty in flood modeling has been addressed by many researchers in the form of equifinality (Beven, 2006) using the generalized likelihood uncertainty estimation (GLUE) procedure e.g. (Aronica et al., 1998; Pappenberger et al., 2005). The main idea is that spatially distributed input and calibration data will help in improving the accuracy of the hydrodynamic models. Remote sensing is particularly well suited for spatial parameterization of the river corridors (Mertes, 2002). Remote sensing input may consist of a Digital Terrain Model (DTM) derived from photogrammetry, or airborne laser scanning (ALS) (Mandlburger et al., 2009). Model boundary conditions of water levels and discharge can be derived from RADAR and meteosat data using a rainfall runoff model. Model output is also regularly calibrated using RADAR-derived flood extent (Schumann et al., 2009). In these ways remote sensing data may help in reducing the overall uncertainty in model predictions.

An important source of uncertainty is the floodplain roughness parameterization (FRP). FRP is a daunting task given the number of processes involved in energy dissipation (Kouwen and Li, 1980) and the spatial heterogeneity of the floodplain vegetation. Floodplain roughness is often parameterized by a single roughness value (Horritt and Bates, 2002), or derived from a remote sensing-based land cover map linked to a lookup table (Van der Sande et al., 2003). Meanwhile, airborne laser scanning (ALS) has proven its ability to accurately map vegetation height (Cobby et al., 2001; Straatsma and Middelkoop, 2007), and hydrodynamic vegetation density (Straatsma, 2008). This allowed the computation of the spatial-temporal roughness coefficient during flood events, instead of a fixed roughness value based on a lookup table (Mason et al., 2003; Mason et al., 2007; Straatsma and Baptist, 2008). Even though the uncertainty in the classified land cover map and the vegetation structural prediction is known, an assessment of the effects of these parameters on the output of hydrodynamic models is rarely carried out.

Floodplain roughness, together with the roughness of the main channel, is often used for model calibration (Horritt and Bates, 2002). Because roughness is changed afterwards anyway, little effort has been spent on the question how accurate it should be parameterized in the first place, and what is the effect of errors in the floodplain roughness parameterization. Werner et al. (2005) assessed the number of classes that should be distinguished for floodplain roughness. Calibration of these models was carried out based on flood extent and water levels. They concluded that

5 classes suffice, but do not address the effects of classification errors, nor did they assess the accuracy of the vegetation parameters that these classes were meant to represent. A few studies have investigated the sensitivity of water levels to the variation in vegetation pattern (Stolker et al., 1999; Huthoff and Augustijn, 2004). Both studies used a 1D river schematization and applied arbitrary changes in vegetation patterns. No studies have been carried out using a two dimensional model, which has a better spatial representation of the roughness and real remote sensing-based roughness parameterization. It is concluded that no comprehensive assessment exists of the effects of uncertainty in floodplain roughness on hydrodynamics

Land cover classification is the primary step for FRP (Geerling et al., 2007; Straatsma and Baptist, 2008), but it leads to a number of errors. Firstly, no classification is perfect. It is always associated with a particular classification accuracy. Overall classification accuracy of ecotope maps typically ranges between 70 and 90 % (Townsend and Walsh, 2001; Geerling et al., 2007; Knotters and Brus, conditionally accepted). Secondly, within a class some natural variation in vegetation structure will occur, which is lost in the classification. This so called within class structural variation can still influence the flow pattern as the water flow is reduced in e.g. the denser parts of the forest, compared to the more open parts. Finally, classification is scale dependent (Van der Sande et al., 2003). Small areas would be classified as a different class, were a finer scale chosen. Examples include single trees in a meadow, or open areas inside a forest.

Our aim is to quantify the uncertainty in 2D hydrodynamic models from remotely sensed roughness parameterization separated in these three error sources, which we will refer to as (1) classification error, (2) within class structural variation, and (3) scale errors. With this study we will lay the foundation for implementing the uncertainty of floodplain roughness in a operational setting.

The study is carried out in the Netherlands in the distributaries of the river Rhine, a lowland alluvial river. We used aerial images as primary remote sensing data. Modeling is carried out using the WAQUA 2D hydrodynamic model (RWS, 2007). Uncertainty is evaluated based on differences in computed roughness values, water levels and flow velocities, and distribution of discharge over different river branches. This is a follow up study of the FC2015 project reported by Straatsma and Alkema (2009). This research was carried out within the Flood Control 2015 program. For more information please visit http://www.floodcontrol2015.com.

2. Roughness parameterization

Accurate predictions of water levels are relevant for the height of the embankments, informing the communities on possible evacuation and for risk assessment. At this moment there is no quantification of the required accuracy of the model output. For hydrodynamic models the vegetation roughness is one of the determining factors for the computed water levels, in addition to bathymetry, roughness of the main channel and the downstream water level. The order of magnitude of the error in water level is reported in several studies. Stolker et al. (1999) modeled differences in water level using a 1D model. Assuming floodplains covered with meadows, the land cover was varied over a length of 10 km with different vegetation types and a cover percentage varying between 10 % and 100 %. Table 1 summarizes the results. For example, in case 10 % of the land cover in the floodplain is changed from meadow to reed over a 10 km stretch of river, the peak increase in water level is 15 cm. Huthoff and Augustijn (2004) report an 8 cm change in water level and stress the effect of the shape of the cross section of the river. Both studies represent a sensitivity study as the sensitivity of the model is tested for variation in input, but they are not studies of error propagation as their input is hypothetical.

Table 1 Effect of classification errors relative to meadows (Stolker et al. 1999)

Land cover change meadow to:	10 % changed to new vegetation cover (cm)	100 % changed to new vegetation cover (cm)
Forest and shrubs	12-20	50-120
Reed	15	50
Herbaceous vegetation	1-6	5-20

2.1 Roughness models

Roughness determines the retardance of the water flow. The higher the roughness, the slower the water will flow and, hence, the higher the water levels will reach. For the non-vegetated river bed, the roughness depends on the grain size and bed form dimensions (Van Rijn 1994) . Vegetation roughness of the floodplains has been described by many different models (Petryk and Bosmajian, 1975; Kouwen and Li, 1980; Kouwen, 2000; Baptist et al., 2007; Huthoff et al., 2007). It depends on vegetation structural characteristics like vegetation height and density, rigidity of the stems and the presence of leaves. Vegetation density is defined as the sum of the projected plant areas in side view per unit volume (m^2m^{-3}, which reduces to m^{-1}). Seasonal variation and management that allows vegetation to vary dynamically lead to a high spatiotemporal variation of vegetation structural characteristics and inherent roughness patterns (Baptist et al., 2004; Jesse, 2004; Van Stokkom et al., 2005).

In any case the base data for roughness parameterization consists of a vegetation map of the floodplain area. Various remote sensing data may provide information on vegetation type and structure including their dynamics. Promising sensor systems include airborne laser scanning (ALS), optical systems and microwave sensors. An important issue to overcome is the translation of remote sensing information, e.g.

the intensity and patterns of reflected electromagnetic radiation to relevant parameters to compute patterns of hydrodynamic roughness.

2.2 Roughness parameterization in WAQUA

The implementation of roughness in hydrodynamic models varies. For WAQUA, the required data for model input has been made available by the Ministry of Public Works, Transport and Water Management (RWS) in the Baseline 4.03 database (Hartman and Van den Braak, 2007). It contains a complete dataset of base maps, derived maps, and a model schematization for the Rhine branches. The hydrodynamic roughness is implemented in a very detailed form in the Baseline database. For WAQUA, hydrodynamic roughness is derived from point, line, and polygon information (Fig. 1).

Roughness polygons are derived from the ecotope map, which is combined with the outline of the main channel, lakes and high water free areas. All these maps are converted using a lookup table to determine the roughness-polygon map (Fig. 1). Each roughness code for vegetation is linked to vegetation structural parameters, such as vegetation height and density plus bottom roughness and drag (Van Velzen et al. 2003). The roughness in the WAQUA model, expressed as Chézy C, depends on the water depth and is computed during runtime of the model using the equation presented in Klopstra et al. (1997). The roughness is assigned to the model computational cell and the energy loss is computed over the cell.

Point and line elements of roughness are derived from a database containing hedges, individual trees and tree-lined lanes. These files are compiled in the Digital Topographic Dataset of the wet infrastructure (DTB-nat). Hedges are parameterized as line elements, assigned with a height and a density, whereas single trees are represented as point data with tree diameter as relevant hydrodynamic parameter. The energy loss of these roughness elements is computed, and attributed to the cell boundary containing the roughness elements.

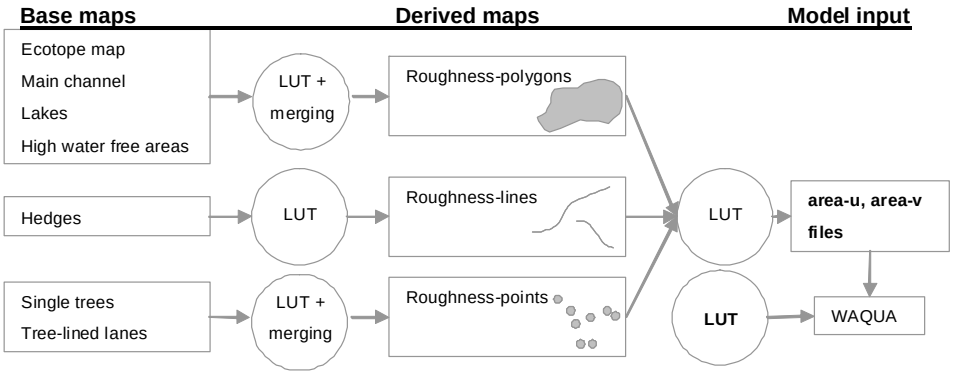

Figure 1 Flow chart of roughness parameterization for the WAQUA hydrodynamic model. The elements that were varied in this study are the immediate model input. The area-u and area-v files have been varied according to the classification accuracy table (Knotters et al. 2008). The lookup table ("rough.karak") relating the derived maps to the WAQUA input has been changed based on field measurements.

The final model input to WAQUA consists of “area files” that describe the roughness in the downstream and the across stream direction (u and v). These files describe for each cell the fraction of the cell that is occupied with a specific roughness code, and the fraction of the cell that is covered by that roughness code. Another lookup table “rough.karak” links the roughness codes to vegetation parameters.

3 Study area

Within this study, we looked at the distributaries of the river Rhine in the Netherlands, excluding the estuary. At the Dutch-German border, the river Rhine has an average discharge of 2250 m^3/s, draining a catchment area of 165 000 km^2. Coming Germany, the river Rhine bifurcates into the "Pannerdensch Kanaal" and the Waal river at the "Pannerdensche Kop" (PK) bifurcation point where roughly one third enters the "Pannerdensch Kanaal" and two thirds are conveyed into the river Waal. At the "IJsselkop" (IJK) bifurcation points again, one third enters the right hand channel named the IJssel river and two thirds flow into the Nederrijn river (Fig. 2). However the exact ratio of dividing the water over the channels depends on the shape and roughness of the main channel and the floodplain.

The study area spans three distributaries with an average water gradient of 0.10 m/km and a maximum length of 152 km along the river axis, which is for the IJssel. The total embanked area amounts to 440 km^2, the floodplain area is 320 km^2 out of which 48 km^2 consists of lakes and side channels. The vegetated area takes up 62 % of the total embanked area. Groynes fixate the main channel and limit the width of the main channel to 250, 160, 105 m for the Waal, Nederrijn and IJssel river. The cross-sectional width between the primary embankments varies between 0.5 and 2.6 km. Meadows dominate the land cover, but recent nature rehabilitation programs led to increased areas with herbaceous vegetation, shrubs and forest.

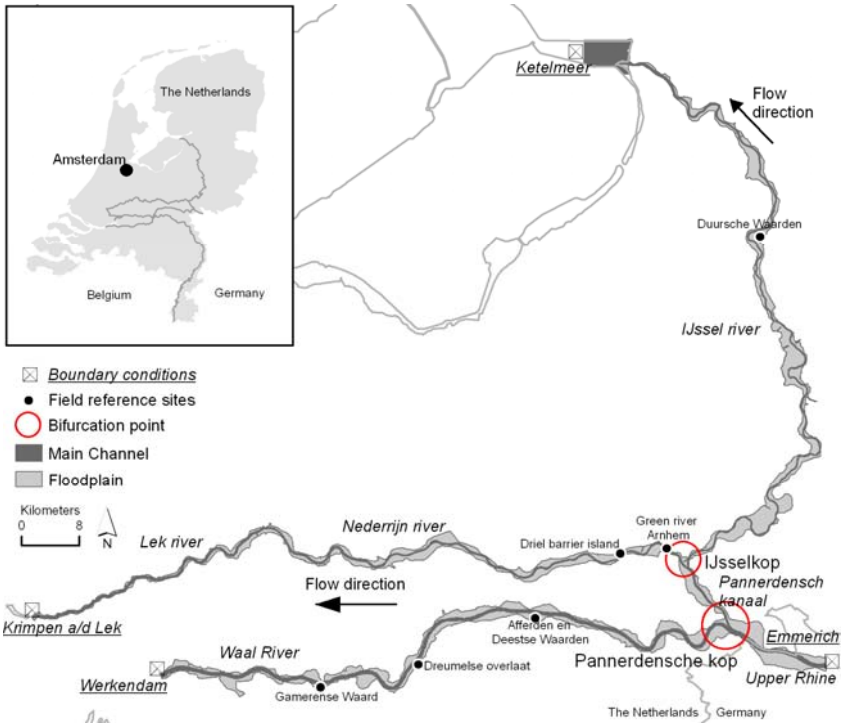

Figure 2 Study area showing the three main distributaries of the river Rhine; Waal, Nederrijn/Lek and IJssel river. At the bifurcation points "Pannerdensche Kop" and "IJsselkop" the water is distributed over the three branches.

4 Methods

In this study, we focused on three aspects of the roughness parameterization and the uncertainty assessment in the WAQUA hydrodynamic model. Firstly we established the relationship between the classification accuracy and the uncertainty in the predicted water levels. Secondly, we determined the effect of the within class variation, and thirdly we determined the hydrodynamic effects of the scale error. For each of the error sources, we carried out 15 model runs of the Rhine distributaries. The uncertainty was determined by the variation in roughness, flow velocities, water levels and discharge distribution.

4.1 Classification error

Currently the vegetation map of the lower Rhine and Meuse floodplains is based on ecotopes. Ecotopes are 'spatial landscape units that are homogeneous as to vegetation structure, succession stage and the main abiotic factors that are relevant to plant growth' (Van der Molen et al., 2003). Mapping of ecotopes within the lower Rhine floodplain is based on visual interpretation and manual classification of vegetation units from aerial photographs, scale 1:10,000 (Jansen and Backx, 1998) . Uncertainty in classification of the terrestrial ecotopes of the Rhine branches has been determined by Knotters et al. (2008) as map purities, the percentage of the mapped area that is correctly classified. The map purities table is similar to the confusion matrix, or error matrix, of a regular classification validation, except that the percentage of the total map that is correctly classified instead of the number of field reference points are listed in the cells. The map purities sum up to one per row. The map purity for the ecotope map of the Rhine branches of 2005 is estimated at 37% for 41 in the field distinguished different ecotopes (n=406 field observations). The overall accuracy of this map is 69% when aggregated to eight terrestrial ecotope groups (Knotters and Brus, conditionally accepted). Classification accuracy is the number of correctly classified points divided by the total number of points in a regular classification. For the map purity table, it is the percentage of the map correctly classified divided by the total map area. In the map purity table (e.g. table 2) the classification accuracy is computed by the sum of the values on the diagonal divided by the sum of the the whole table.

A few problems were noted with the fieldwork related to the discernability of the different ecotopes in the field. Also, the spatial support of the field data (point measurements) did not match the aerial image interpretation of ecotopes per polygon, sized 400 m^2 or more. Therefore the reported classification accuracy should be interpreted as a minimum value.

4.1.1 Recoding the area-files as realizations of vegetation types

The method to create new realizations of the roughness maps has been presented in Straatsma and Alkema (2009), and will be iterated here in brief. In that research, we used the map purities table as probabilities that an ecotope polygon is classified correctly. We computed the cumulative probability by summing up the probabilities along each row in the map purities table (Fig. 3). For each polygon in the ecotope map, we drew a random number between zero and one with a uniform distribution,

and using the cumulative probability we assigned a new ecotope code to each of the polygons (Fig. 3). This procedure was repeated 15 times for each polygon, giving 15 new realizations of the original ecotope map. Each has the same probability and can be seen as different outcomes of the same manual procedure of creating the ecotope map. These maps were recoded to WAQUA roughness codes and used in the 2D hydrodynamic model with a stationary discharge.

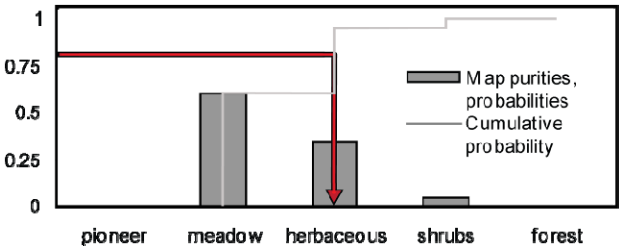

Figure 3 Recoding based on the cumulative probability function derived from the map purities. map purities are for a meadow polygon. The red arrow gives the random number of for a meadow (0.81) and the subsequent recoding into herbaceous vegetation as the random number is between 0.6 and 0.95.

Contrasting with the 2009 study, we worked on the WAQUA roughness files ("area-u.001" and "area-v.001"; Fig. 1) directly to bypass the labour intensive conversions from ecotope maps to roughness files. These area-files are ASCII formatted column files that list the WAQUA grid cell coordinates, the roughness code and the fractional coverage of that code with respect to the total cell area. To be able to change all the WAQUA cells that are within a single roughness polygon, the polygon-ID had was added to the area files. The additional advantage was that the update of the roughness files are more up to date than the ecotope map of 1997 provided in the Baseline-4 database. In 2003, a large update of the roughness map was carried out, but these updates were not implemented in a new ecotope map. Therefore the ecotope map still reflected the situation of 1997, while the area files included the update of 2003.

The map purity table of Knotters et al. (2008) has been standardized by Straatsma and Alkema (2009). In this study, we aggregated the map purity table to the vegetation types according to the vegetation handbook of Van Velzen et al. (2003) (Table 2). This was done by computing a weighted average over the lines of the ecotopes that are within the same vegetation class and summing up the columns that represent the same vegetation class. Weights were assigned based on the surface area of the ecotopes that were merged into a single vegetation type. Correct classifications are present in the diagonal of the map purity table, indicated in grey in table 1. Related to Fig. 3, an ecotope polygon representing production meadow would have a 52 % chance of keeping its vegetation type and a 48 % chance of being recoded to another vegetation type (Table 1).

The recoding of polygons was carried out for each polygon individually and repeated 15 times resulting in 15 new area-u and area-v files. These realizations represent 15

possible outcomes of the ecotope map given the validation presented in Knotters et al. (2008).

Table 2 Purity matrix for (aggregated) ecotopes in the Rhine branches (based on (Knotters et al., 2008)). Also the total areas of the different ecotopes are given (ref km^2: coverage of ecotopes in reference situation, after PM km^2: coverage of ecotopes after application of the purity matrix, dA: change in surface area due to application of the purity matrix). Users accuracy is 37% at ecotope level, 69 % ecotope group level (eight classes) and 43 % at vegetation types level (16 classes presented here).

Description	Roughness code	ref Km2	after PM Km2	dA Km2	Groyne field / sand bar 111	Buildup area / paved 114	Agricultural area 121	Pioneer vegetation 1250	Production meadow 1201	Natural grass/hayland 1202	Dry herbaceous veg. 1212	Reed-grass 1804	Reed 1807	Softwood shrubs 1231	Willow plantation 1232	Thorny shrubs 1233	Softwood production forest 1242	Hardwood forest 1244	Softwood forest 1245
Equivalent roughness length																			
Groyne field / sand bar	111	3.4	4.1	+0.7	86%									14%					
Stone protection	113	0.5	0.0	-0.5		80%								20%					
Buildup area / paved	114	13.8	18.2	+4.4		92%			5%					2%			2%		
Agricultural area	121	35.3	32.9	-2.5			78%		21%										
Submerged vegetation (grass-type)																			
Pioneer vegetation	1250	0.8	2.5	+1.7	53%	24%		8%		15%									
Production meadow	1201	135.4	102.8	-32.6	1%		2%		52%	32%	7%			3%			3%		
Natural grass/hayland	1202	71.8	77.8	+6.0		1%	2%	2%	33%	43%	8%	3%	5%				2%		
Submerged vegetation (reed-type)																			
Dry herbaceous veg.	1212	22.4	29.9	+7.5		10%	2%	4%	2%	8%	53%	4%	2%	5%	5%	4%	2%		
Reed-grass	1804	3.7	3.7	0.0						22%	59%			16%					3%
Reed	1807	3.4	6.8	+3.4								26%	65%	9%					
Emergent vegetation																			
Softwood shrubs	1231	4.0	11.1	+7.1					3%	3%	10%		3%	43%		12%	16%	1%	8%
Willow plantation	1232	0.1	1.0	+1.0															100%
Thorny shrubs	1233	1.6	2.3	+0.7		9%				5%	16%			20%		21%	2%	10%	16%
Softwood product. forest	1242	2.6	8.7	+6.2		12%			6%							8%	43%		31%
Hardwood forest	1244	5.9	2.1	-3.8		30%								12%			12%	32%	15%
Softwood forest	1245	11.2	12.0	+0.8							6%			11%		3%			79%

4.1.2 Dependence of uncertainty in water levels on classification accuracy

The validation of the ecotope map was disputed due to the difference in support between field data and aerial image interpretation and some of the ecotope types were not discernable from one another based on the plant communities. Therefore the true accuracy of the ecotope type is not known. The reported accuracy is assumed to be a minimum, given the classification accuracies reported in other studies that vary between 70 % and 92 %.

In anticipation of a future undisputed validation of the ecotope map, we wanted to establish the relationship between the classification accuracy of the ecotope map and the uncertainty in the peak water levels. This relation may also assist water managers in setting a benchmark for classification accuracy for the ecotope map given the uncertainty in water levels.

To determine the uncertainty in water levels, we created three new map purity tables that represent the classification accuracy at ecotope group level of 80, 90, and 95% based on the current table that has a 69% classification accuracy. The new map

purity tables were created by increasing the values on the diagonal and decreasing the values off-diagonal in the map purity table using the following method. The off diagonal values were decreased by a manually chosen multiplication factor between 0 and 1. For each line in the matrix, the difference between the original off-diagonal values and the new values was added to the diagonal value. This led to the increase in the diagonal value and decrease of the off-diagonal values, leading to a new error matrix with a higher classification accuracy. The ecotope map purity matrix was subsequently aggregated into 8 ecotope group classes and 16 vegetation type classes. The multiplication factor was changed by trial and error until the classification accuracy at ecotope group level was 80, 90, and 95% (Table 3).

Table 3 Characteristics of classification accuracies.

Set	Classification accuracy at ecotope group level	Classification accuracy at vegetation type level	Number of runs in WAQUA
1	69 %	43 %	15
2	80 %	65 %	15
3	90 %	83 %	15
4	95 %	92 %	15

At each accuracy level 15 new realizations were created of the two roughness files (area-u and area-v), and for each of the realizations a new random number was drawn for each of the polygons giving a completely independent realization of the roughness distribution within the constraints of the map purity table. In total 60 WAQUA runs were carried out to determine the effect of the increasing classification accuracy on the uncertainty of the water levels. The variation of the water levels between the different runs is the main output of the uncertainty analysis.

4.2 Within class variation of vegetation structural characteristics

Contrary to the classification accuracy, the error in the lookup table is generally not well-known. Popular guidelines on selecting roughness values e.g. (Chow, 1959; Arcement and Schneider, 1989) give Manning's values, without taking the water depth into account, and only make a weak link to vegetation structure. Ecotopes are defined as being uniform in vegetation structural characteristics and from the modeling perspective there is no within class variation, similar to other guidelines on selecting roughness values. However, large variations in vegetation height and density were measured in the field (Straatsma and Ritzen, 2002).

Some remote sensing techniques, like terrestrial and airborne laser scanning, have the capacity to map the spatial distribution of vegetation height and density. For example, the variation within a single forested ecotope may range between 0 and 0.35 m^{-1} (Fig. 4), which was mapped using terrestrial laser scanning (Straatsma et al., 2008). This spatial differentiation of vegetation structural characteristics inside ecotopes is not incorporated in the ecotope map, nor in WAQUA.

Van Velzen et al. (2003) provided a complete lookup table with all the relevant vegetation parameters. They also provide a list of field reference sites and their measured vegetation structure for each vegetation class. It is clear from this list that the variation in vegetation structure is large and that the class values are based on

only a few measurements. The error in the lookup table is therefore largely unknown. Fig. 5 shows the fixed values for vegetation height and density in the lookup table incorporated in Baseline and in the "rough.karak" lookup table (Fig. 1).

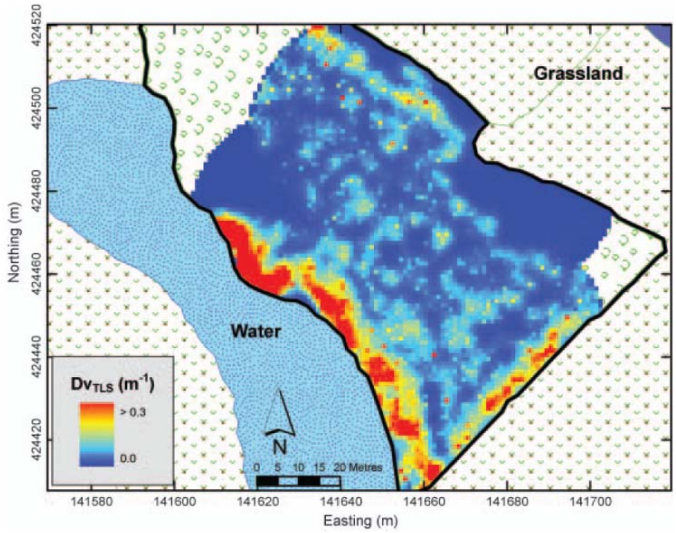

Figure 4 Within class variation of vegetation density in a forested ecotope in the Gamerensche Waard. Dv_{TLS} is the vegetation density as modelled using terrestrial laser scanning data (from Straatsma (2008).

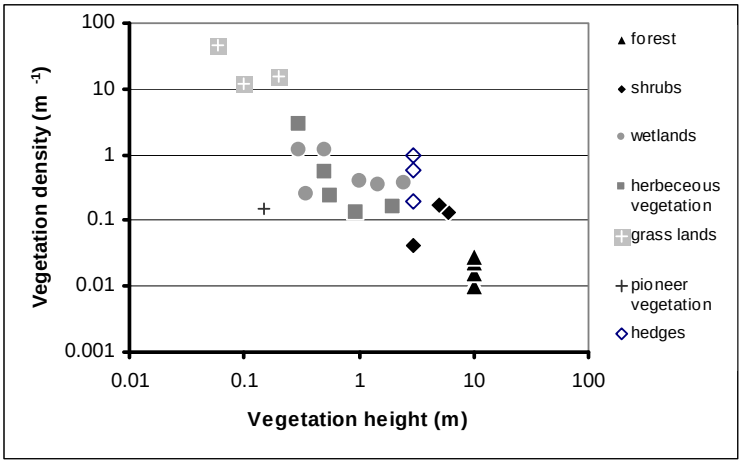

Figure 5 Feature space of vegetation height and density of different vegetation types in the vegetation handbook.

The maximum uncertainty in the water levels due to this so called within class variation was determined by Straatsma and Alkema (2009). They compiled a database of field vegetation measurements, categorized them per vegetation type and computed the quartiles of the vegetation height and density independently. Combinations of minimum vegetation height and density up to maximum vegetation height and density were chosen to determine the maximum range in uncertainty at peak water levels. While these combinations effectively show maximum uncertainty, these combination are not realistic as an inverse relationship exists between

vegetation height and density. Taller vegetation is in general more open than lower vegetation. Therefore, in this study realistic combinations of vegetation height and density are computed to determine a realistic uncertainty in water levels due to within class variation at the design discharge in 2015 (16 000 m^3/s).

4.2.1 Within class variation of vegetation structural characteristics per vegetation type

The challenge is to determine realistic values for within class variation. Two different types of within class variation are discernable: within ecotopes and within vegetation types of the vegetation handbook of Van Velzen et al. (2003). Ecotopes are aggregated into vegetation types during Baseline preprocessing of WAQUA model input. Therefore, we focused on within class variation within the vegetation types of the handbook.

To fill in the knowledge gap on within class variation, we analyzed the database of vegetation structural parameters that was compiled by Straatsma and Alkema (2009) based on fieldwork in Dutch floodplains in winter between 2000 and 2007. This data is available on request. As WAQUA does not work with roughness maps as input directly, but with roughness codes, a new set of codes was compiled that describe the variation in vegetation structural characteristics per vegetation type of Van Velzen et al. (2003). Four new variations were chosen for each vegetation type.

For submerged vegetation, the vegetation height and density need to be given. For a number of classes, enough field data were present in the database and in that case the following procedure was followed. Data were divided in four classes, each containing an equal number of field reference measurements. The data were first divided by the median value of the vegetation density, and subsequently each of these two classes were subdivided by the median value of vegetation height. The mean and standard deviation were computed for the resulting four variations. In the majority of the cases, however, not enough field data was available, and the vegetation handbook was used as the starting point. The values for vegetation height and density that were chosen for these cases were based on expert judgement and the known distribution of vegetation parameters from similar vegetation types that did have enough field data. In general the four classes were made up by multiplying the height and density by 0.5 and 2.0 (Fig. 6). The different combinations of these values give a skewed distribution around the original value that mimics the distribution as seen in the database.

For emergent vegetation, the vegetation density values were divided in quartiles, and the mean and standard deviation was computed. Again, in case not enough data was available, the density was based on the vegetation handbook. Variation was applied by multiplying the density by 0.25, 0.5, 2, and 4. Vegetation height of emergent vegetation was maintained as it was at a height of 10 m.

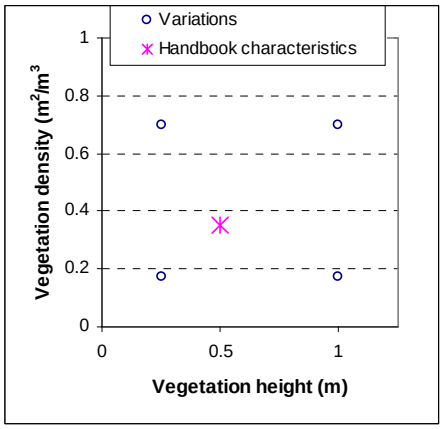

Figure 6 Variations in vegetation structural characteristics based on the handbook values and multiplication factors of 0.5 and 2.0 for vegetation height and density.

4.2.2 Implementation in WAQUA

In WAQUA, the vegetation structure is attributed to each grid cell by using a lookup table that relates to a roughness code to relevant surface characteristics. The codes with values between 1201 and 1400 are reserved for different vegetation types. Normally, only 25 codes are in use in this range. For this study, we enlarged the lookup table to 100 items, giving four possible variations of the vegetation structure of that vegetation type, see appendix B.

Updating the current WAQUA input needs to incorporate the within class variation. The spatial distribution of the roughness types is stored in files called *area-u* and *area-v*. These ASCII formatted column files contain the MN coordinates of the computational grid, the roughness code and the fraction of the cell covered with that code. Each roughness code between 1201 and 1400 was assigned one of the variations that were described above. Variations were assigned randomly, which is warranted by the fact that each of the classes contain an equal number of field plots and may be considered equally probable. For example, a cell that is partially covered by dry herbaceous vegetation has the code 1212 in Baseline 4 in the original column file. In the new *area-u* file one of the codes ranging between 1258 to 1261 will be assigned (Box 1). Codes 1258 to 1261 represent the variation. This will result in a new set of roughness files with a random component in the spatial distribution of the vegetation structure. An example is given in box 1, appendix B gives the full rough.karak file for those classes that were varied in this study.

Baseline 4 roughness code

```
r_code = 1212 a = 0.56 b = 0.23 c = 1.8 d = 0.1 # Dry herbaceous vegetation
```

Variations including within class variation

```
r_code = 1258 a = 0.89 b = 0.067 c = 1.8 d = 0.1 # Dry herbaceous vegetation
r_code = 1259 a = 0.59 b = 0.128 c = 1.8 d = 0.1 # Dry herbaceous vegetation
r_code = 1260 a = 0.81 b = 0.034 c = 1.8 d = 0.1 # Dry herbaceous vegetation
r_code = 1261 a = 0.44 b = 0.021 c = 1.8 d = 0.1 # Dry herbaceous vegetation
```

Box 1. Example of the currently used roughness file and the variations that include the within class variation, see also appendix B.

Roughness codes between 1801 and 1900 consist of compound classes, describing a mixture of two other classes. These compound classes cover 2.5 % of the vegetated flood plain area and 1 % of the total embanked area. For example, roughness code 1807 is reed with 25 % open area and refers to code 1226 (reed) and code 122 (mulch). For each of these vegetation types, four new variations were created in which the reference to the dominant vegetation type is changed to the new variations of that dominant type.

Roughness codes between 111 and 122 refer to unvegetated areas, such as paved areas, agricultural lands, or mulch. For these classes, only a Nikuradse roughness length is given in the lookup table. For each of the original classes, four new classes were created with varying roughness lengths using multiplication factors of 0.6, 0.8, 1.3 and 1.6. These multiplication factors were chosen to achieve similar variation in roughness heights for the unvegetated area's as for production meadow. In Fig. 7 the equivalent roughness heights for production meadow if the density and height of the vegetation is varied by factors 0.5 and 2 (black lines). The central thick red line depicts the reference roughness height of the vegetation for the standard values for height and density. The dashed red lines show the roughnesses if the reference roughness is multiplied by factors 0.6, 0.8, 1.3 and 1.6.

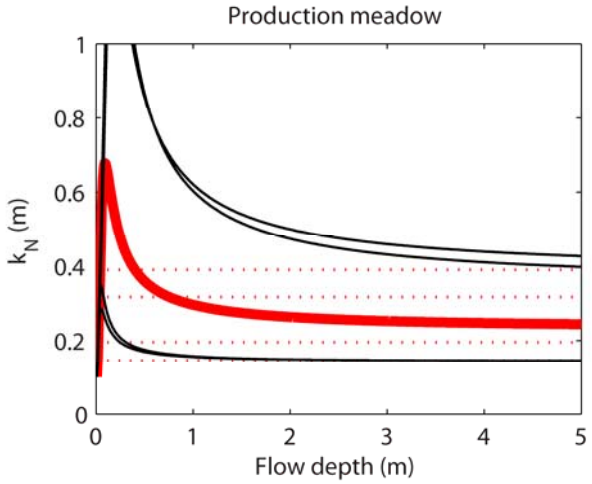

Figure 7 Determination of multiplication factors for unvegetated areas based on production meadow. Thick red line shows the variation of the k_N values with water depth according to Klopstra et al. (1997). The solid black lines show the meadow roughness with higher and lower vegeation height and density. The four dashed red lines are the fixed roughness values based on the multiplication factors that coincide with the changes in roughness for meadows.

To be able to determine the effect of this random component on the variation of the hydrodynamics, fifteen new sets of roughness files were prepared. Each of these was used as input to the same model with the same boundary conditions. Results were compared based on the predicted water levels on the river axis of the three main distributaries of the river Rhine and the discharge distribution over the bifurcation points. A steady state discharge of 16 000 m^3/s was chosen which is the same as the design discharge of the Rhine for the year 2015.

4.3 Scale error

The ecotopes were mapped at a scale a scale of 1:10,000 (Jansen and Backx, 1998). The minimum polygon size digitized for the ecotope map was 20 by 20 m, while the median polygon size is 5000 m^2, and occasionally terrestrial ecotopes may cover more than 3 km^2. In the recoding as carried out for the determination of the effects of the classification error, the polygon size remains unchanged. However classification is scale dependent (Van der Sande et al., 2003; Addink et al., 2007), and large polygons may contain small patches that could be classified as a different ecotope.

The field validation was carried out with point measurements (Knotters et al., 2008), while aerial image classification was carried out following a decision tree per polygon (Jansen and Backx, 1998). This difference in support and scale can be used in determination of the scale errors in the ecotope map. We used the same map purities table to determine the uncertainty at a different scale. We standardized the size of the polygons to the smallest polygon mapped from the images by overlaying the ecotope map with the curvilinear computational grid of WAQUA with a median cell size of 700 m^2. The overlayed map has a median polygon size of 575 m^2, approximating the minimum mapping area for the ecotope map, 400 m^2. In doing so, we implicitly assumed that the support of the field measurements would equal the size of the overlayed polygons. An additional reason for standardizing the polygon size is that for larger ecotopes, more spatial information is available to the interpreter and we can assume that assigning an erroneous ecotope is less likely for larger polygons.

Recoding was carried out using the same method as for recoding for the classification error. Also for this error source, 15 realizations were created.

4.4 Hydrodynamic modeling

The WAQUA model has been used by the Dutch Ministry of Transport, Public Works and Water Management for the two-dimensional simulation of hydrodynamics in the complex channel and floodplain areas of the Rivers Rhine and Meuse in the Netherlands (RWS, 2007) . For the present study, a series of simulations of steady flow in the study area was carried out. The WAQUA model that was used for this study is based on a staggered curvilinear grid. Each of the 886,861 cells represents a column shaped volume of water with a variable surface area of 700 m^2 on average. The water flow between the water volumes in the raster is calculated by numerically solving the Saint-Venant equations of mass balance and of convective and diffusive motion in two dimensions (RWS, 2007) using a finite difference method. The boundary conditions of the model are the river discharge at the upstream boundary, and the water level at the downstream boundary using a discharge-stage relationship. Input data from which the WAQUA model calculates the water flow field are a Digital Terrain Model (DTM), barriers and a roughness map. We ran WAQUA with a discharge of 16,000 m^3/s at the upstream end at Emmerich, Germany. Water levels at the downstream end were around 4.39, 2.02 and 0.42 m above ordnance datum for the downstream boundary conditions of the Waal, Nederrijn-Lek and IJssel rivers respectively. The exact water level being governed by

a rating curve. The full model of the Rhine branches was run as proximity of the boundaries to the bifurcation points would limit the effect of water level variations.

We ran six sets of 15 model runs. The first four sets were related to the classification accuracy at 69, 80, 90, and 95% classification accuracy at ecotope group level. The fifth was related to the within class variation and the sixth to the scale error. The number of model runs was limited as the time required for individual runs amounted to eleven hours or more on a linux computational cluster of 10 processors. Output of these sets that were used to determine the uncertainty were:

- Spatially distributed values of the standard deviation of the Nikuradse equivalent roughness length
- Spatially distributed values of the standard deviation of the flow velocities
- Variation of the peak water levels along the river axis for each of the three distributaries (Bovenrijn-Waal, Pannerdensch Kanaal-Nederrijn-Lek, IJssel). The variation is summarized by the spread (84 percentile minus 16 percentile) and range of water levels at each river kilometer to determine the spatial variation of the uncertainty.
- Discharge distribution between the branches at the Pannerdensche Kop and IJsselkop bifurcation point.

5. Results

Before we show the hydrodynamic effects of the classification error, within class variation and the scale error, we present the analysis of the within class variation based on the database compiled by Straatsma and Alkema (2009).

5.1 Overview of within class variation in the vegetation structural characteristics per vegetation type

The compilation of the field data resulted in a database of 445 field measurements, based on reference data from six floodplain sections: Duursche Waarden, Afferdensche en Deestse Waarden, Groene rivier Arnhem, Gamerensche Waard, Driel barrier island, Dreumelse overlaat (Fig. 1) (Straatsma and Alkema, 2009). For six different vegetation types, the database contained enough data to compute the vegetation structure for four different classes. Fig. 8 gives the parameter space for vegetation height and density for submerged vegetation. The class means (big black dots) were used in the lookup table for these classes. For herbaceous vegetation and natural grass and hayland the class mean of the vegetation density is roughly half and twice the median value which is indicated by the dashed vertical line. For softwood shrubs, no combination of high density and high vegetation height existed in the database. These results were at the basis of lowering the vegetation height data for some of the classes. For example, hairy willowherb has a vegetation height of 1.0 m in the vegetation handbook, but a vegetation height of 2 m would be unrealistic. Therefore a maximum height of 1.3 m was chosen.

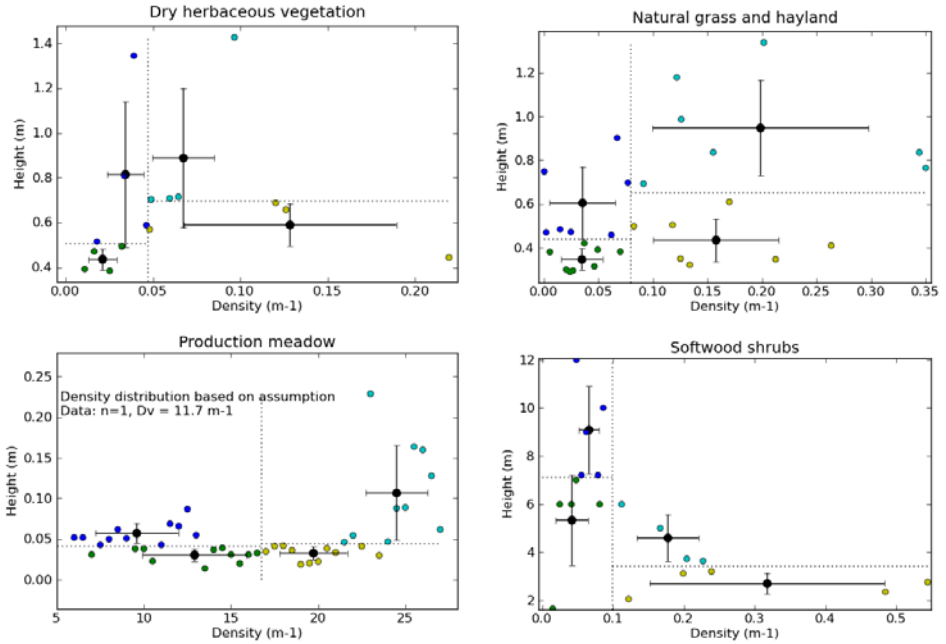

Figure 8 Variation of vegetation height and density for submerged vegetation types. The dotted lines give the class boundaries. The large sized dots represent the class mean, the error bars give the standard deviation for vegetation density (horizontally) and vegetation height (vertically).

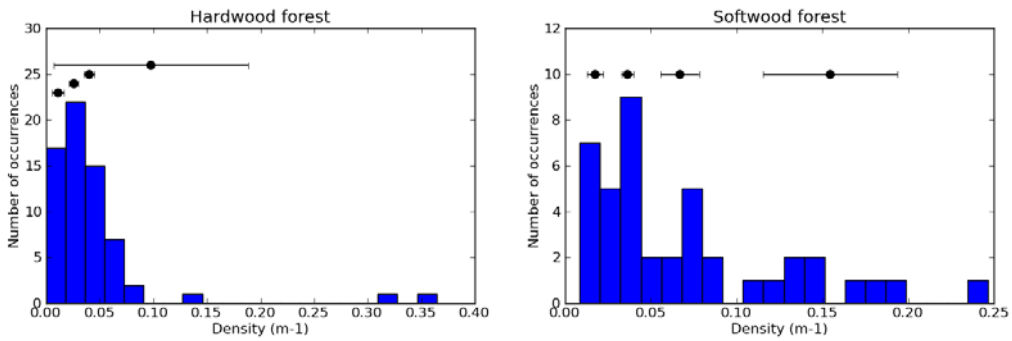

Figure 9 Histograms of vegetation density for hardwood and softwood forest. Black dots give the class mean. Standard deviation indicated as horizontal bars (vertical shift for visualisation only).

The distribution of vegetation density in forests shows a skewed distribution (Fig. 9). For hardwood forest values as high as 0.3 to 0.35 (m^{-1}) were found, but these are more indicative of shrubs. The fact that these values are still present in the forest vegetation type is an indication of classification errors in the ecotope map. Based on these distribution, we decided to use the multiplication factors of 0.25, 0.5, 2, and 4 for the forest types that did not have enough field reference data. Vegetation height of forest is always set to 10 m, an arbitrary value that is at least more than the maximum water depth. The overview of the vegetation structural parameters is given in Table 4.

Table 4 Vegetation types of the handbook and the within class variation. Each of the cells in the area-u and area-v files that contained one of the roughness codes between 1201 and 1400 was updated with a randomly chosen roughness code that contained the values in the last four columns.

Vegetation type[a]	Structural characteristic[b]	Baseline 4 Code	Handbook Values	Within class variation[c] 1	2	3	4
Production meadow	Dv	1201	45.000	12.909	9.591	19.727	24.500
	Hv		0.06	0.03	0.06	0.03	0.11
Natural grass and hayland	Dv	1202	12.000	0.035	0.035	0.158	0.199
	Hv		0.10	0.35	0.60	0.43	0.95
Herbaceous meadow	Dv	1203	15.000	7.500	7.500	30.000	30.000
	Hv		0.20	0.10	0.40	0.10	0.40
Thistle herb. Veg.	Dv	1211	3.000	1.500	1.500	6.000	6.000
	Hv		0.30	0.15	0.60	0.15	0.60
Dry herbaceous vegetation	Dv	1212	0.230	0.021	0.034	0.128	0.067
	Hv		0.56	0.44	0.81	0.59	0.89
Brambles	Dv	1213	0.560	0.280	0.280	1.120	1.120
	Hv		0.50	0.25	1.00	0.25	1.00
Hairy Willowherb	Dv	1214	0.130	0.065	0.065	0.260	0.260
	Hv		0.95	0.48	1.30	0.48	1.30
Reed herb. Veg.	Dv	1215	0.160	0.080	0.080	0.320	0.320
	Hv		2.00	1.00	4.00	1.00	4.00
Wet herb. Veg.	Dv	1221	0.250	0.125	0.125	0.500	0.500
	Hv		0.35	0.18	0.70	0.18	0.70
Sedge	Dv	1222	1.200	0.600	0.600	2.400	2.400
	Hv		0.30	0.15	0.60	0.15	0.60
Reed-grass	Dv	1223	0.400	0.200	0.200	0.800	0.800
	Hv		1.0	0.5	2.0	0.5	2.0
Bulrush	Dv	1224	1.200	0.600	0.600	2.400	2.400
	Hv		0.50	0.25	1.00	0.25	1.00
Reed-mace	Dv	1225	0.350	0.175	0.175	0.700	0.700
	Hv		1.50	0.75	3.00	0.75	3.00
Reed	Dv	1226	0.370	0.185	0.185	0.740	0.740
	Hv		2.50	1.25	3.50	1.25	3.50
Softwood shrubs	Dv	1231	0.130	0.042	0.066	0.318	0.177
	Hv		6.00	5.33	9.08	2.70	4.59
Willow plantation	Dv	1232	0.041	0.021	0.021	0.082	0.082
	Hv		3.00	1.50	6.00	1.50	6.00
Thorny shrubs	Dv	1233	0.170	0.085	0.085	0.340	0.340
	Hv		5.00	2.50	10.00	2.50	10.00
Hardwood prod. forest	Dv	1241	0.011	0.003	0.006	0.022	0.044
	Hv		10.0	10.0	10.0	10.0	10.0
Softwood prod. forest	Dv	1242	0.028	0.007	0.014	0.056	0.112
	Hv		10.0	10.0	10.0	10.0	10.0
Pine forest	Dv	1243	0.016	0.004	0.008	0.032	0.064
	Hv		10.0	10.0	10.0	10.0	10.0
Hardwood forest	Dv	1244	0.023	0.011	0.026	0.040	0.098
	Hv		10.0	10.0	10.0	10.0	10.0
Softwood forest	Dv	1245	0.028	0.018	0.036	0.067	0.155
	Hv		10.0	10.0	10.0	10.0	10.0
Orchard low	Dv	1246	0.024	0.012	0.012	0.048	0.048
	Hv		3.0	1.5	4.0	1.5	4.0
Orchard high	Dv	1247	0.010	0.005	0.005	0.020	0.020
	Hv		6.0	3.0	9.0	3.0	9.0
Pioneer vegetation	Dv	1250	0.150	0.075	0.075	0.300	0.300
	Hv		0.15	0.01	0.04	0.07	0.14

[a] Types in italics are based on field reference data, other types are based on the vegetation handbook, multiplication factors and expert judgment.

[b] Dv is vegetation density (m^2/m^3), Hv vegetation height (m)

[c] Four variations based on either database analysis, or multiplication of the values in the vegetation handbook. The values in italics are exceptions to these method, in these cases the vegetation height was lowered.

5.2 Hydrodynamic effects

5.2.1 Variation in roughness

Each realization of the roughness files leads to a different pattern of roughness in the floodplain as the ecotope polygons, or cells are recoded based on the map purity table. As an example, Fig. 10 shows 4 out of the 15 roughness maps for two floodplain sections based on the classification error at a 69 % classification accuracy at ecotope group level. At this classification accuracy many of the polygons are recoded into a different vegetation type and that shows in large areas that change in roughness. For example in the Nederrijn at km 920, 5 km upstream of Wijk bij Duurstede (not on map), a large production meadow is situated on the southern floodplain. This area has a low roughness in three out of the four presented roughness maps, but one map shows a significantly higher roughness as an orange color. The Millinger Waard floodplain section (right hand panels) is a nature development area that consists of smaller ecotopes, and hence the changes are also spatially less extensive. Still, large differences are found in Nikuradse equivalent roughness length. For example in the upstream part, the area outside of the summer embankment shows large differences in roughness at a small spatial scale. The changes in roughness in this area is specifically relevant due to the proximity of the bifurcation point, therefore small changes in roughness immediately change the distribution of the water over the distributaries.

To show the local variation in roughness the spread in the roughness values has been computed by taking the difference between the 84 percentile and the 16 percentile of the Nikuradse roughness lengths at each location. The spread was computed for each error source. Fig. 11 shows the difference between the classification error at 69 % accuracy, within class variation and the scale error for the Millinger Waard floodplain section. When looking at the natural levee east of river kilometer 872, a large variation is visible for the classification error, a smaller spread for the within class structural variation and a patchy structure for the scale error. In general, the spread in roughness is smallest for the within class variation, spread in roughness is the same for classification error and scale error, but for the realizations of the scale error, the shifts in roughness are less spatially correlated due to the small polygon size.

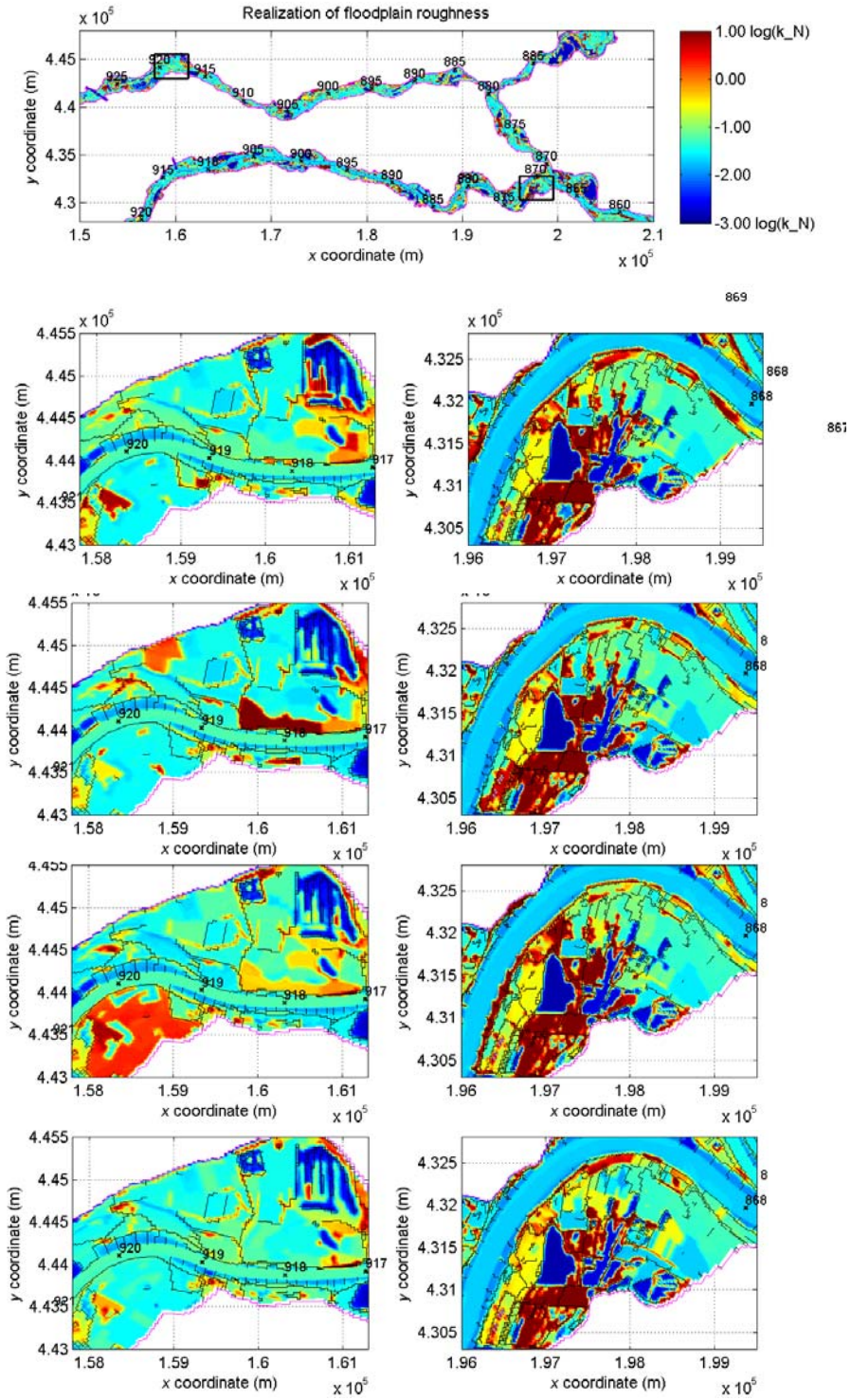

Figure 10 Roughness values for four realizations based on the classification error at 69 % classification accuracy. Note the large shifts in the agricultural area in the Nederrijn floodplain section (left hand panels) and the more small scale changes in the nature development area of the Millinger Waard floodplain section (right hand panels).

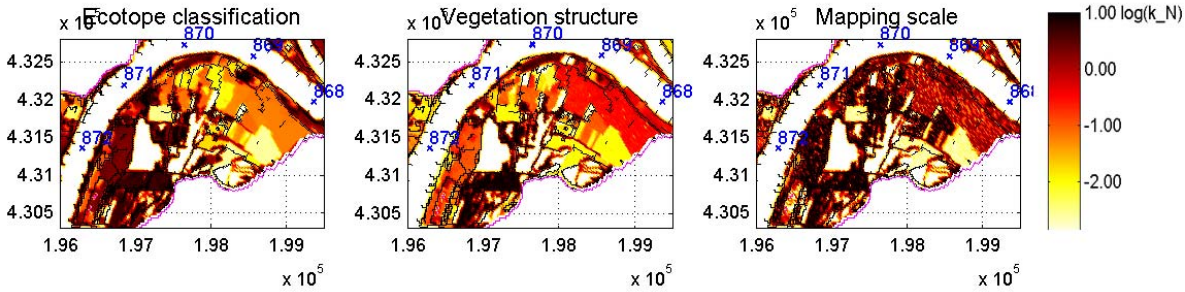

Figure 11 Local spread in effective roughness heights (log k_N-values), based on the 15 realizations of roughness maps for three error sources: ecotope classification (69% accuracy), within class structural vegetation, and mapping scale.

5.2.2 Spatially distributed values of the standard deviation of the flow velocities

Variations in roughness have a strong effect on the flow velocities in the floodplains and to a lesser extent in the main channel. Fig. 12 shows the spread in the flow velocities in the same two floodplain sections along the Nederrijn and the Waal as Fig. 10. A comparison with the roughness variations revealed that, in general, flow variations are largest where roughness variations are largest. However, as some parts of the floodplain contribute only little to the conveyance of the river, in these parts large roughness variations have only little effect on flow velocities. The strongest variations in flow velocities are typically found at locations where water flows away from or into the main river channel. The upstream end of the Millinger Waard floodplain section exemplifies the point as the spread in the flow velocities is more than 0.2 m/s.

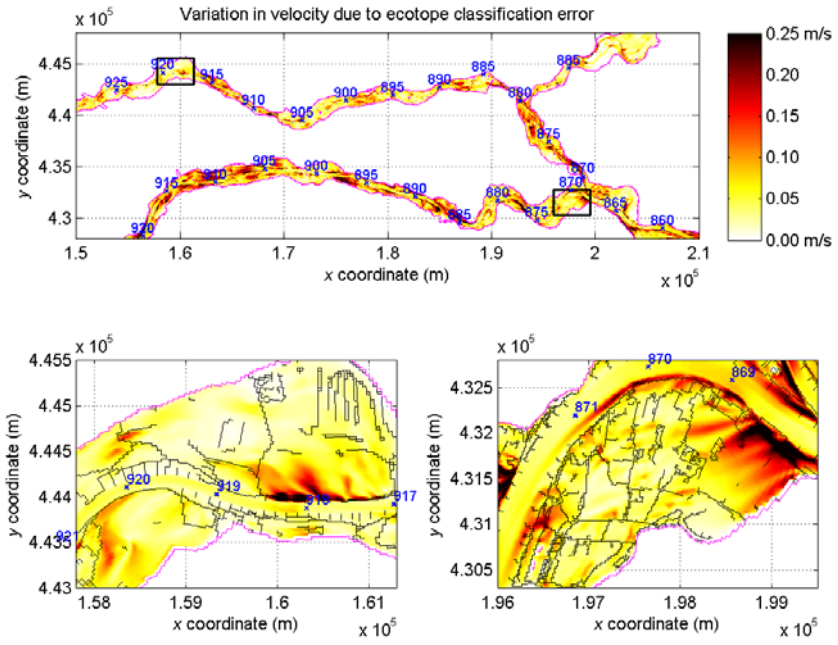

Figure 12 Spread in flow velocities in two floodplain sections based on the classification error at 69 % accuracy.

When comparing the three main error sources (Fig. 13) it becomes apparent that the classification error has the largest effect on the flow velocities with a spread of up to 0.25 m/s. Within class variation has only a small effect on the flow velocities of maximum 0.10 m/s locally. Scale error takes the intermediate position. Remarkably, flow velocities due to the classification error at 95 % classification error (not shown) are still larger than the spread due to scale error and within class variation.

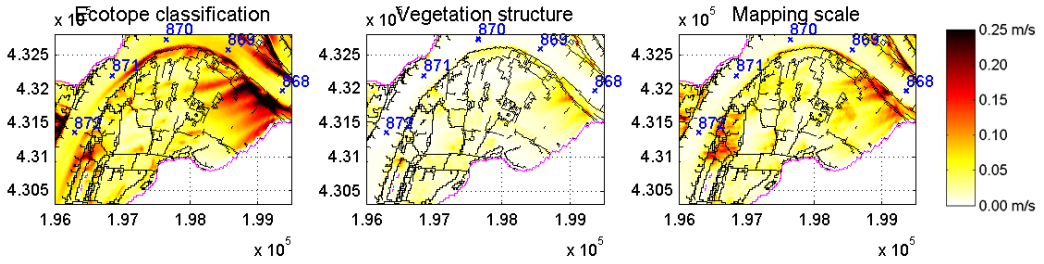

Figure 13 Spread in flow velocities in the Millinger Waard floodplain section based on the classification error (69 % accuracy), within class variation, and scale error. Largest variation in flow velocity was found for the uncertainty from the classification error, smallest uncertainty resulted from the within class variation.

5.2.3 Variation of the peak water levels

Classification error

Water levels vary due to the different realizations. We show the effect of the different roughness maps on the water levels at the axes of the distributaries. Fig. 14 gives the outcome of the individual runs as thin grey lines. Data has been summarized for the following river sections: (1) Bovenrijn-Waal (BRWA), (2) Pannerdensch Kanaal-Nederrijn-Lek (PKNELE), and (3) IJssel (IJ). The variation is summarized by the range and spread in water levels for each river kilometer at the river axes (Fig. 14, 16). The zero level in these graphs represents the average predicted water level at that river kilometer. For each run, the deviation from this average has been depicted to optimize interpretation of the results.

Classification accuracy exerts a strong influence on the water levels in the study area (Fig. 14). For the three distributaries, the variation between the individual runs decreases as shown by the thin grey lines for the individual runs, and as summarized by the spread and the range. Note that the variation at the model boundaries is limited due to the applied discharge-water level relationship. The variation of the water level at the boundaries resulted purely from the variation in discharge. For the Bovenrijn-Waal, the median spread drops from 0.07 to 0.02 m due to the increase in classification accuracy of 69 to 95 %, while the maximum spread decrease from 0.2 to 0.05 m (Table 5, Fig. 15). For the IJssel, the values are 0.13 to 0.05 m for median spread and 0.3 down to 0.12 for the maximum spread (Fig. 14, Table 5). The Pannerdensch Kanaal-Nederrijn-Lek distributary takes an intermediate position.

The Waal shows a relatively linear decrease in the spread, both median and maximum, with the increase in classification accuracy (Fig. 15), the statistics for the IJssel display linear decrease in the median value, but even at a 90 % classification accuracy, the maximum in the spread still reaches 0.28 m (Table 5; Fig. 15). The

interquartile range in the spreads even increases from 80 to 90 % classification accuracy. This resulted from the locally larger variation in roughness in the 90 % classification realizations, enabled by the independent drawing of random numbers for each realization.

Table 5 Overview of the uncertainty in water levels due to different error sources. The values represent the spread in water levels at peak discharge between 15 model runs.

		Spread Bovenrijn-Waal (m)	Spread Pannerdensch Kanaal-Nederrijn-Lek (m)	Spread IJssel (m)	Spread all Rhine distributaries (m)
Median spread	Classification accuracy at 69%	0.069	0.103	0.138	0.114
	Classification accuracy at 80%	0.065	0.081	0.093	0.081
	Classification accuracy at 90%	0.039	0.065	0.082	0.059
	Classification accuracy at 95%	0.020	0.045	0.051	0.038
	Within class variation	0.005	0.005	0.007	0.006
	Scale error	0.015	0.016	0.022	0.017
Maximum spread	Classification accuracy at 69%	0.197	0.192	0.285	0.285
	Classification accuracy at 80%	0.105	0.120	0.278	0.278
	Classification accuracy at 90%	0.089	0.129	0.279	0.279
	Classification accuracy at 95%	0.048	0.075	0.118	0.118
	Within class variation	0.008	0.012	0.023	0.023
	Scale error	0.029	0.029	0.038	0.038

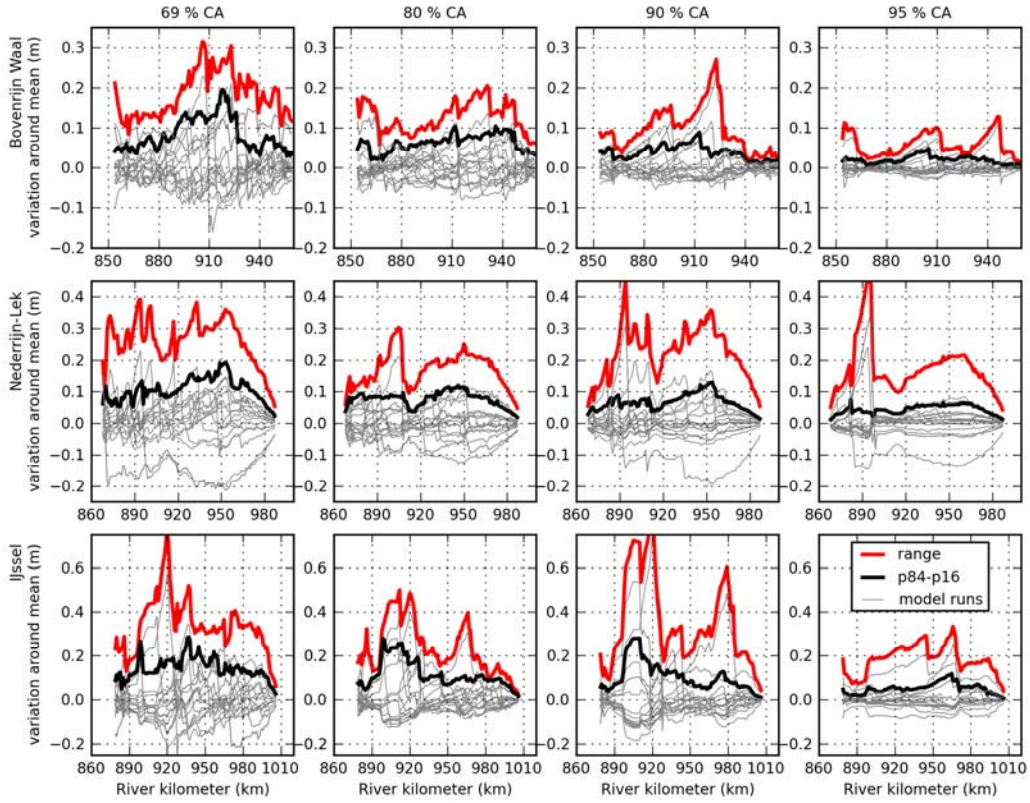

Figure 14 Variations in water levels due to different classification accuracies for the Rhine distributaries. Note the differences in the vertical scale between the rows of figures.

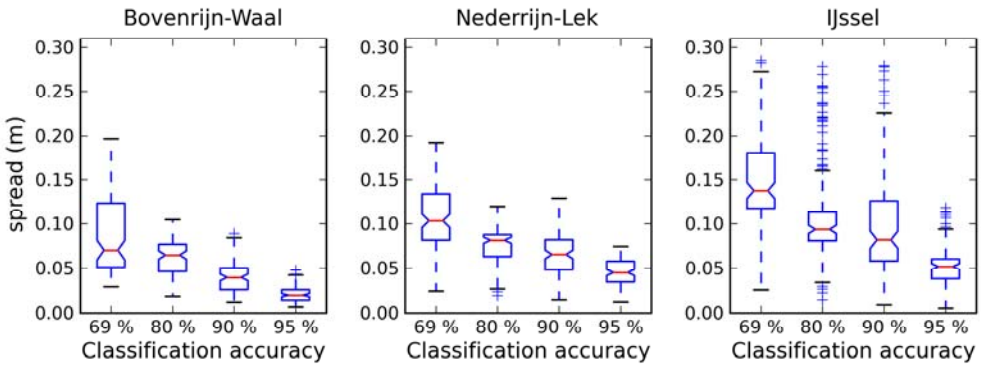

Figure 15 Box plot of the spreads in water level over the three Rhine distributaries. Each black line in Fig. 14 becomes an individual box here. The spread clearly decreases with increasing classification accuracy. The median spread is given by the red line. The box extends from the interquartile range, whiskers show the range of 1.5 times the interquartile range, and the flier points are the points beyond the whisker range.

Within class variation and scale error

Similar to the effects on flow velocity, the uncertainty in water levels due to within class variation and scale error is much smaller than for classification error (Fig. 16, Table 5). Within class variation leads to a maximum spread of 0.023 m, and a median spread of 0.006 m. This shows that if the average value of the lookup table is correct, variations around the average of up to a factor four for submerged vegetation and a factor 16 for emergent vegetation lead to a 6 mm uncertainty in water levels. Scale error has a larger effect of the uncertainty in the water levels, up to 4 cm in spread.

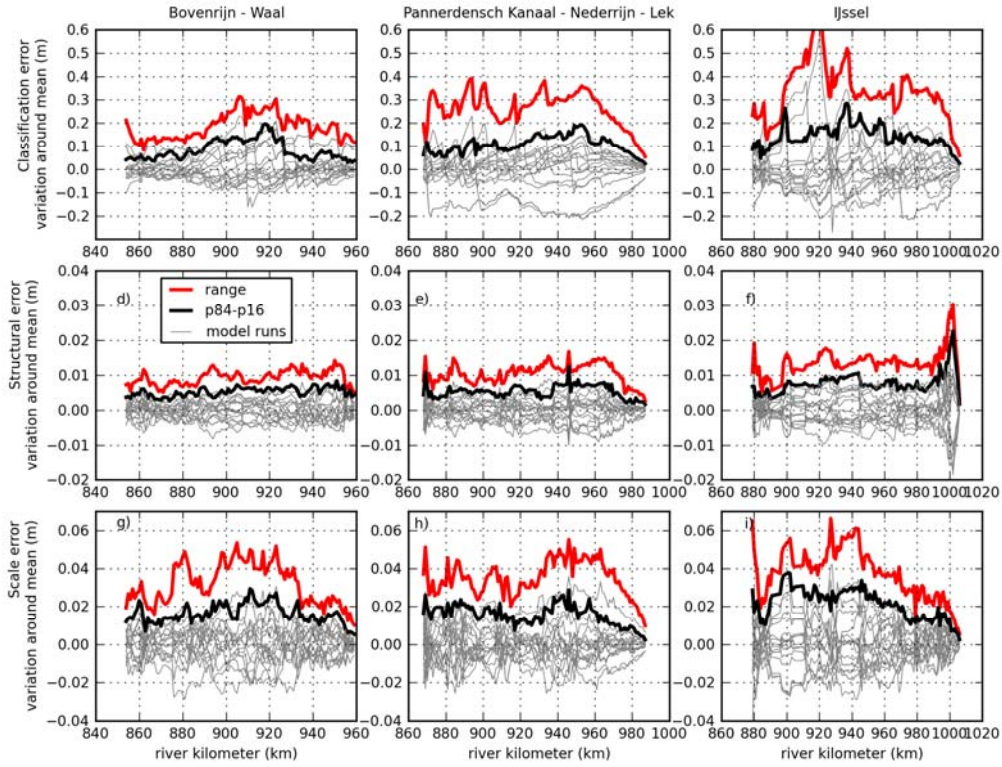

Figure 16 Variations in water levels due to different error sources for the three river distributaries: (a-c) classification accuracy, (d-f) within class variation, and (g-i) scale error. Note the differences in the vertical scale between the rows of figures. Classification error is given for comparison and equals the first column in Fig. 14.

To summarize the sources of uncertainty, Fig. 17 shows the spread for all distributaries together. This graph clearly shows that classification accuracy if the dominant source of uncertainty in water levels. Even at a 95 % classification accuracy, the uncertainty due to classification error is larger than the within class variation and the scale error.

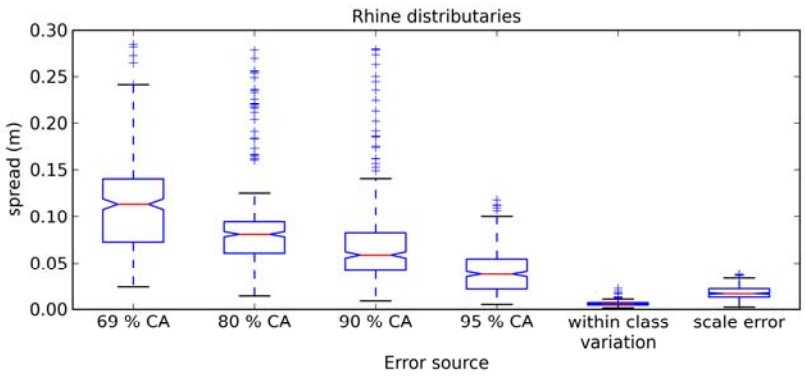

Figure 17 Comparison between uncertainty due to different error sources of floodplain vegetation. Classification error is the dominant source of uncertainty. Even at the 95 % classification accuracy at ecotope group level.

5.2.4 Discharge distribution over the bifurcation points

The variation in roughness also influences the distribution of the water at the bifurcation points. Lower roughness leads to a lower water level locally which will increase the conveyance in that branche. The area directly downstream of the bifurcation points exerts the highest influence on the discharge distribution. Classification error shows the largest effect on the discharge distribution. Even at a 95 % classification accuracy, the spread in the discharge is twice the spread for scale error and around four times the spread for within class variation (Table 6). A lower discharge at the bifurcation point will influence the water levels in the whole distributary. A good example of this effect is the Nederrijn-Lek at a 69 % classification accuracy (Fig. 14b), showing two model runs that are consistently lower than the other runs.

The spread in the discharge distribution decreases with increasing classification error, similar to the water level. The range in the discharge distribution is more prone to outliers. For example at 95 % classification accuracy, one run shifted a large discharge (170 m^3/s) from the Nederrijn to the IJssel. These shifts in discharge may have a large effect on the water levels (Fig. 18). A 200 m^3/s increase in discharge raised the water levels with approximately 0.05 m at the model boundaries (Werkendam, Krimpen aan de Lek, Ketelmeer, Lobith; Fig. 18, Fig. 2), but locally the increase may be as high as 0.25 m at the IJsselkop.

Table 6 Spread in discharge distribution (p84-p16 percentile) of different stochastic errors (m3/s). In brackets the range in the discharge variation. In brackets the range in discharge for each distributary. Statistics based on 15 model runs.

	Spread Bovenrijn-Waal (m^3/s)	Spread Pannerdensch Kanaal (m^3/s)	Spread Nederrijn-Lek (m^3/s)	Spread IJssel (m^3/s)
Classification accuracy at 69 %	93 (391)	69 (367)	104 (215)	114 (260)
Classification accuracy at 80 %	104 (205)	104 (179)	76 (181)	66 (99)
Classification accuracy at 90 %	51 (91)	39 (88)	62 (218)	40 (190)
Classification accuracy at 95 %	29 (51)	22 (45)	51 (174)	26 (176)
Vegetation structural variation	8 (13)	6 (14)	5 (8)	8 (11)
Scale error	18 (27)	13 (32)	11 (38)	13 (23)

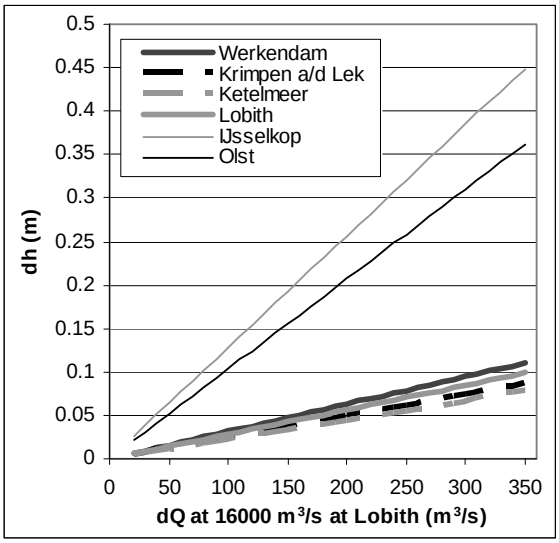

Figure 18 Dependence of difference in water level on difference in discharge for four boundary water level stations in the Rhine distributaries (dQ-dh relationship at design discharge). Variation in discharge may due to changing roughness patterns around the bifurcation points may explain up to 0.10 m in water level.

5.3 Number of runs

Because of the computational demands of the WAQUA model of the Rhine branches, in the current study the number of individual runs was limited to 15 per set, totaling 90 runs, and four weeks of computation time on 6 cores of a Linux computational cluster. The question arises whether enough runs were done to reliably estimate the spread in water levels. For that reason, we assessed the maximum spread per distributary (Fig. 19). It appears that the variation in the spread stabilizes after around 13 model runs. Fifteen model runs are therefore suggested for future probabilistic studies. This number of runs is acceptable if spatially-averaged results are required (average uncertainty along distributary), or to get a rough indication of the spread in water levels at a specific section in the river. Therefore, we also looked at the maximum spread in 5 km long sections, the grey lines in Fig. 19. Also at the scale of a river section, the spread in the water level levels off after around 13 model runs, even though small changes in spread occasionally happen in the 14th , or 15th run. This implies that to get a more reliable uncertainty range at a particular location

in the river, for example to asses the effects of a planned local river engineering measure, more simulation runs would be necessary.

The low number of runs also affected the results on the classification error, where the maximum spread did not show a linear decrease with increasing classification error. If 500 runs were carried out, the estimate of the spread would have been more robust and it is expected that the maximum spread would also show a linear relation with classification accuracy. However that was beyond our computational capacities.

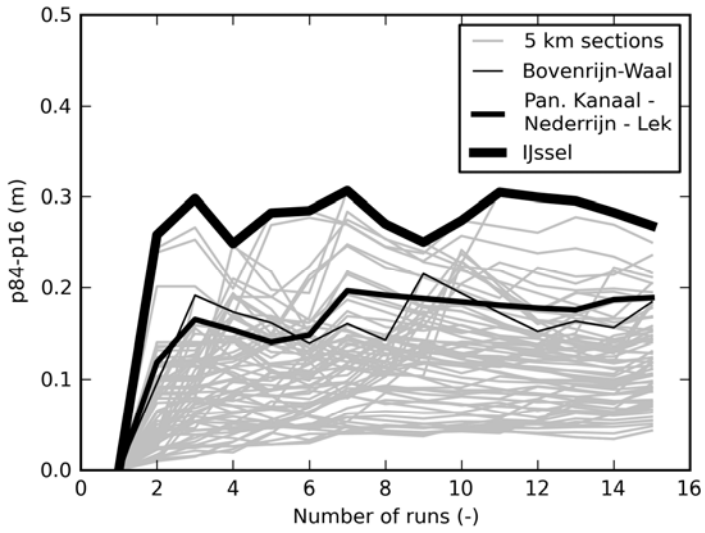

Figure 19 Variation of the spread as a function of the number of runs for the three distributaries and 5 km sections. The spread stabilizes after 13 runs for classification accuracy at 69 % classification accuracy.

6. Discussion

In the previous section, we looked at the hydrodynamic effects due to different error sources related to vegetation roughness in floodplains. This is the first study to assess the uncertainty from floodplain roughness parameterization in a 2D model, with the error sources broken down into three different sources. The study allows ranking of the relative importance of the three uncertainty sources on resulting uncertainty in flood levels. In general, the effects on flood levels are relatively large when compared to the accuracy required for the hydraulic boundary conditions in the Netherlands. For landscaping measures the effect should be less than 2 mm rise in water level at the river axis and less than 5 m^3/s change in discharge distribution over the bifurcation points. However, one should view the results presented here in the context in which numerical river models are commonly applied in flood defense studies. The hydraulic roughness in these models is typically calibrated using historical flood events. Next, the design water levels are estimated by extrapolating the calibrated roughness parameterizations to high discharge situations. The uncertainty range that is presented in the current study corresponds to the situation where a river model is built up from available roughness parameterizations, and that no additional calibration steps are applied. Therefore, the uncertainty range presented here can be drastically reduced if calibration steps are included in the model construction procedure. In a follow-up study we will focus on obtaining uncertainty bounds around flood water levels and discharge redistribution if calibration steps are also applied.

The pivot point for the methodology is the validation of the ecotope map presented in Knotters et al. (2008) and Knotters and Brus (conditionally accepted). The overall classification accuracy was low, 69 % at ecotope group level, but has been disputed due to differences in support and discernability of the different ecotopes in the field. The classification error, based on the current map purity table, led to a large spread in water levels. However, other studies of vegetation classification, showed higher accuracies based on automated classification algorithms (Van der Sande et al., 2003; Geerling et al., 2007; Straatsma and Baptist, 2008). It was expected that a manual delineation and classification of floodplain vegetation would results in a higher classification accuracy. The large effect of the classification error on the water levels and discharge distribution points at the need for an undisputed and complete quality assessment of the ecotope map. Given the limitations, the uncertainty should be interpreted as a maximum.

In the present study we linked a 69 % classification accuracy to a maximum spread in water levels is 0.20, 0.19 and 0.29 m for the different river sections. For a higher classification accuracy the variation in water levels reduced to 0.05, 0.07, and 0.12 m at a 95 % classification accuracy. Based on this relation a political choice can be made about the accepted amount of uncertainty that the river manager is willing to allow for the water levels. This uncertainty in water levels can then be translated into a required classification accuracy. A tangible benchmark for classification accuracy that is substantiated by research would be a stimulation for the remote sensing

community to provide the optimal method to reach this goal. Primary aim of any method should be to increase the classification accuracy.

The within class variation in four classes that was applied randomly to the roughness files resulted in a cm variation in water levels. This is a rather small effect compared to classification errors. However, in assigning the vegetation structural characteristics only little field data was available for most classes. Preferably, a complete database would ground the choices for the lookup table and the within class variation. Alternatively, ALS data can provide vegetation structural characteristics directly (Cobby et al., 2001; Straatsma and Middelkoop, 2007). Such methods remove the within class variation, and replaces it with a known prediction error, which could be the base for a subsequent sensivity analysis. The downside is the cost of ALS, and the need for such a new method can only be warranted with increased classification accuracy. The current uncertainty assessment may help in setting benchmarks for the desired accuracy. However, we showed that classification accuracy is the dominant source of uncertainty, the uncertainty due to the within class variation is an order of magnitude smaller than for classification error. Still high confidence is placed on the accuracy of the vegetation structural values in the lookup table. When there is a bias in these values, the water levels could change much more than based on the present assessment.

Scale error is the uncertainty that would result from a mapping exercise at a larger scale. It proves that the uncertainty can be reduced to a large extent if the map would be made with smaller polygons, resulting from the larger scale map. In practice, this is unlikely as even at a larger scale, many of the meadows would still be mapped as a single large polygon, as little spatial variation is present in the area due to the land management, such as mowing. In the map validation, this should be taken into account, otherwise large polygons would be equally easily recoded into another vegetation type as small polygons. The interpreter has more information available to make the classification for larger polygons than for smaller polygons. Therefore it is likely that the classification accuracy is higher for larger polygons. During a map validation, the dependence between polygon size and classification accuracy should therefore be established.

The habitual parameter to calibrate a hydrodynamic model is the roughness of the main channel. This study shows the possible range in water levels that result from assuming that the floodplain roughness is not correct. In theory, it would be possible to calibrate a flow model on different ecotope distributions as well in a probabilistic manner. Given a discrepancy between model outcome and measured values of water level, or flow velocities, different ecotope distributions can be tested against the measured values. The obvious disadvantage is that no direction for searching can be defined beforehand, making the calibration process more time consuming.

The complex system of hydrodynamics that we try to capture in a model has many uncertainties (location, level, and nature, sensu Walker et al. (Walker et al., 2003)). In this study, we quantified the effects of spatial variability of vegetation roughness. Within the ongoing project of uncertainty reduction within Flood Control 2015 other

aspects are captured, such as morphological changes at the bifurcation points, design discharge and operational discharge prediction. The uncertainties of these other sources should be compared in a final study.

The quantification of the uncertainty in water levels and discharge distribution will help to make more realistic decisions as the error bands are substantiated. These are still relative differences and not absolute accuracies of the model output after calibration, but it may serve as a first step. It can also influence the assessment of the height of the embankments as insight is given in the variability of the outcome of the flow models at design discharge. Moreover, the error bands may serve as an incentive to quantify the desired accuracy in the vegetation structural characteristics. This means that an upper limit can be put on the variation in water levels that is accepted from errors in roughness.

7. Conclusions and recommendations.

In this study, the variation in water levels has been studied resulting from three error sources: (1) classification error, (2) within class variation, and (3) scale error. We conclude that:

1. The uncertainty ranges presented in the current study represent maximal values, corresponding to a model that is not calibrated on historical flood events. Accuracies are being improved drastically during calibration of the model.
2. Classification accuracy is the dominant source of uncertainty, within class variation provides the smallest addition to the overall uncertainty.
3. The classification error at polygon level leads to a maximum spread in the predicted water levels per river kilometer of 0.20, 0.19 and 0.29 m for Upper Rhine-Waal, Pannerdensch Kanaal-Nederrijn-Lek and the IJssel river, respectively. Largest effects are found in the IJssel river and the Pannerdensch Kanaal. These values are valid at the current reported classification accuracy of 69 % at ecotope group level.
4. There is an inverse relationship between the classification accuracy and the uncertainty in the water levels. The median of the spread shows a linear relation between classification accuracy and uncertainty in water levels. The maximum spread per distributary is more sensitive to outliers and shows a sharp decrease between 90 an 95 % classification accuracy.
5. The within class variation leads to a maximum spread in water levels of 0.01, 0.015, and 0.02 m for Upper Rhine- Waal, Pannerdensch Kanaal-Nederrijn-Lek and the IJssel river respectively.
6. The scale error leads to a maximum spread in water level of 0.02, 0.03 and 0.035 m for the Upper Rhine- Waal, Pannerdensch Kanaal-Nederrijn-Lek and the IJssel river respectively. These values are an order of magnitude lower then what was found for the classification error, demonstrating the need to unambiguously link map purities to a spatial scale.
7. The spread in the discharge distribution at the Pannerdensche Kop and IJsselkop bifurcation point is maximum 104 and 114 m^3/s respectively for classification error. Effects of within class variation and scale error is ten and five times smaller.
8. Priority should be given to increasing the classification accuracy as this generates the largest error.
9. The suitable number of runs for a probabilistic assessment of classification accuracy might be fifteen when considering river-reach sections. More runs seem necessary if a more local assessment is carried out.

With this study, we explored the relationship between vegetation parameterization and the effects on predicted water levels and identified the relative importance of three floodplain roughness uncertainty sources. The obtained flood level uncertainty ranges represent maximal values as no calibration steps are incorporated in the procedure. Follow-up studies will focus on the importance of model calibration in suppressing uncertainties of simulated values.

Based on these results we recommend to:

1. Establish the relationship between polygon size and classification accuracy
2. Rank the sources of uncertainty, including the uncertainty due to the choice of roughness model.
3. Determine the absolute uncertainty at the design discharge due to uncertain floodplain roughness.
4. Link the uncertainty in floodplain roughness to operational flood forecasting:
   a) Based on the measured discharge and the 1 to 4 day forecast, the relation should be established between discharge and uncertainty
   b) Using the forecasted water levels, an additional error band is computed based on the uncertainty in floodplain roughness. This will show the relative importance of the floodplain roughness with respect to the uncertainty in the forecasted discharge.

References

Addink, E.A., De Jong, S.M., Pebesma, E.J., 2007. The importance of scale in object-based mapping of vegetation parameters with hyperspectral imagery. Photogrammetric Engineering and Remote Sensing 73, 905-912.

Arcement, G.J., Schneider, V.R., 1989. Guide for selecting Mannings n roughness coefficients for natural channels and floodplains. Reston, Virginia, USA.

Aronica, G., Hankin, B., Beven, K., 1998. Uncertainty and equifinality in calibrating distributed roughness coefficients in a flood propagation model with limited data. Advances in Water Resources 22, 349-365.

Baptist, M.J., Babovich, V., Rodríguez Uthurburu, J., Keijzer, M., Uittenbogaard, R.E., Mynett, A., Verwey, A., 2007. On inducing equations for vegetation resistance. Journal of hydraulic research 45, 435-450.

Baptist, M.J., Penning, W.E., Duel, H., Smits, A.J.M., Geerling, G.W., Van der Lee, G.E.M., Van Alphen, J.S.L., 2004. Assessment of the effects of cyclic floodplain rejuvenation on flood levels and biodiversity along the Rhine River. River Research and Applications 20, 285-297.

Bates, P.D., Horritt, M.S., Fewtrell, T.J., 2010. A simple inertial formulation of the shallow water equations for efficient two-dimensional flood inundation modelling. Journal of Hydrology 387, 33-45.

Beven, K., 2006. A manifesto for the equifinality thesis. Journal of Hydrology 320, 18-36.

Charlton, M.E., Large, A.R.G., Fuller, I.C., 2003. Application of airborne LIDAR in river environments: the river Cocket, Northhumberland, UK. Earth Surfaces, Processes and Landforms 28, 299-306.

Chow, V.T., 1959. Open channel hydraulics. McGraw Hill, New York.

Cobby, D.M., Mason, D.C., Davenport, I.J., 2001. Image processing of airborne scanning laser altimetry data for improved river flood modeling. ISPRS Journal of Photogrammetry and Remote Sensing 56, 121-138.

Geerling, G.W., Labrador-Garcia, M., Clevers, J., Ragas, A., Smits, A.J.M., 2007. Classification of floodplain vegetation by data-fusion of Spectral (CASI) and LiDAR data. International Journal of Remote Sensing 28, 4263 – 4284.

Hartman, M.R., Van den Braak, W.E.W., 2007. Baseline manual, baseline 4.03. RIZA, Arnhem, 128.

Horritt, M.S., Bates, P.D., 2002. Evaluation of 1D and 2D numerical models for predicting river flood inundation. Journal of Hydrology 268, 87-99.

Hunter, N.M., Bates, P.D., Horritt, M.S., Wilson, M.D., 2007. Simple spatially-distributed models for predicting flood inundation: A review. Geomorphology 90, 208-225.

Huthoff, F., Augustijn, D., 2004. Sensitivity analysis of floodplain roughness in 1D flow. In: Liong, S.Y., Phoon, S.I., Babovich, V. (Eds.), 6th Interational conference on hydroinformatics, Singapore, Malaysia, pp. 301-308.

Huthoff, F., Augustijn, D.C.M., Hulscher, S.J.M.H., 2007. Analytical solution of the depth-averaged flow velocity in case of submerged rigid cylindrical vegetation. Water Resources Research 43, (W06413).

Jansen, B.J.M., Backx, J.J.G.M., 1998. Ecotope mapping Rhine Branches-east 1997 (in Dutch). RIZA, Lelystad, 41.

Jesse, P., 2004. Hydraulic resistance in (nature) development (in Dutch). RIZA, Arnhem, 65.

Klopstra, D., Barneveld, H., Van Noortwijk, J.M., Van Velzen, E.H., 1997. Analytical model for hydraulic roughness of submerged vegetation. 27th international IAHR conference San Francisco, pp. 775-780.

Knotters, M., Brus, D.J., conditionally accepted. Sampling for validation of ecotope maps of floodplains in the Netherlands. Journal of Environmental Management.

Knotters, M., Brus, D.J., Heidema, A.H., 2008. Validatie van de ecotopenkaarten van de rijkswateren. Alterra, Wageningen, 47.

Kouwen, N., 2000. Friction factors for coniferous trees along rivers. Journal of hydraulic engineering 126, 732-740.

Kouwen, N., Li, R.M., 1980. Biomechanics of vegetated channel linings. Journal of Hydraulics Divisions 106, 1085-1103.

Mandlburger, G., Hauer, C., Höfle, B., Habersack, H., Pfeifer, N., 2009. Optimisation of LiDAR derived terrain models for river flow modelling. Hydrol. Earth Syst. Sci. Discuss 5, 3605-3638.

Mason, D.C., Cobby, D.M., Horrit, M.S., Bates, P., 2003. Floodplain friction parameterization in two-dimensional river food models using vegetation heights derived from airborne scanning laser altimetry. Hydrological Processes 17, 1711-1732.

Mason, D.C., Horrit, M.S., Hunter, N.M., Bates, P.D., 2007. Use of fused airborne scanning laser altimetry and digital map data for urban flood modelling. Hydrological Processes 21, 1436-1447.

Mertes, L.A.K., 2002. Remote sensing of riverine landscapes. Freshwater Biology 47, 799-816.

Pappenberger, F., Beven, K., Hunter, N.M., Bates, P., Gouweleeuw, B.T., Thielen, J., De Roo, A.P.J., 2005. Cascading model uncertainty from medium range weather forecasts (10 days) to rainfall-runoff models to flood inundation predictions within the European Flood Forecasting System (EFFS). Hydrology and Earth System Sciences 9, 381-393.

Petryk, S., Bosmajian, G., 1975. Analysis of flow through vegetation. Journal of Hydraulics Divisions 101, 871-884.

RWS, 2007. Users guide WAQUA: Technical Report SIMONA 92-10. http://www.waqua.nl/systeem/documentatie/usedoc/slib3d/ug-slib3d.pdf,, data accessed 13-02-2008.

Schumann, G., Di Baldasasarre, G., Bates, P.D., 2009. The utility of spaceborne radar to render flood inundation maps based on multialgorithm ensembles. IEEE transactions on geoscience and remote sensing 47, 2801-2807

Stolker, C., Van Velzen, E.H., Klaassen, G.J., 1999. Nauwkeurigheidsanalyse stromingsweerstand vegetatie (in Dutch). Delft Hydraulics, RIZA, Delft, Arnhem, 21.

Straatsma, M.W., 2008. Quantitative mapping of hydrodynamic vegetation density of floodplain forests using airborne laser scanning. Photogrammetric Engineering and Remote Sensing 47, 987-998.

Straatsma, M.W., Alkema, D., 2009. Error propagation in hydrodynamics of lowland rivers due to uncertainty in vegetation roughness parameterization FloodControl2015, 44.

Straatsma, M.W., Baptist, M.J., 2008. Floodplain roughness parameterization using airborne laser scanning and spectral remote sensing. Remote Sensing of Environment 112, 1062-1080.

Straatsma, M.W., Middelkoop, H., 2007. Extracting structural characteristics of herbaceous floodplain vegetation for hydrodynamic modeling using airborne laser scanner data. International Journal of Remote Sensing 28, 2447-2467.

Straatsma, M.W., Ritzen, M.R., 2002. Laseraltimetrie en vegetatieruwheid van uiterwaarden (in Dutch). Physical Geography. Utrecht University, Utrecht, p. 117.

Straatsma, M.W., Warmink, J.J., Middelkoop, H., 2008. Two novel methods for field measurements of hydrodynamic density of floodplain vegetation using terrestrial laser scanning and digital parallel photography. International Journal of Remote Sensing 29, 1595-1617.

Townsend, P.A., Walsh, J., 2001. Remote sensing of forested wetlands: application of multitemporal and multispectral satellite imagery to determine plant community composition and structure in southeastern USA. Plant Ecology 157, 129-149.

Van der Molen, D.T., Geilen, N., Backx, J.J.G.M., Jansen, B.J.M., Wolfert, H.P., 2003. Water Ecotope Classification for integrated water management in the Netherlands. European Water Management Online. http://www.ewaonline.de/journal/2003_03.pdf, data accessed

Van der Sande, C.J., De Jong, S.M., De Roo, A.P.J., 2003. A segmentation and classification approach of IKONOS-2 imagery for land cover mapping to assist flood risk and flood damage assessment. International Journal of Applied Earth Observation and Geoinformation 4, 217-229.

Van Stokkom, H.T.C., Smits, A.J.M., Leuven, R.S.E.W., 2005. Flood defense in the Netherlands a new era, a new approach. Water International 30, 76-87.

Van Velzen, E.H., Jesse, P., Cornelissen, P., Coops, H., 2003. Stromingsweerstand vegetatie in uiterwaarden (in Dutch). RIZA, Arnhem, 131.

Walker, W.E., Harremoes, P., Rotmans, J., Van der Sluijs, J.P., Van Asselt, M.B.A., Janssen, P., Krayer von Kraus, M.P., 2003. Defining Uncertainty A Conceptual Basis for Uncertainty Management in Model-Based Decision Support. Integrated Assessment 4, 5-17.

Werner, M.G.F., Hunter, N.M., Bates, P.D., 2005. Identifiability of distributed floodplain roughness values in flood extent estimation. Journal of Hydrology 314, 139-157.

Appendix A: Names of the ecotopes and associated Baseline 4 roughness codes

Ecotope code	Description	Roughness code baseline 4	Roughness code description
HA-1	Highwater free agriculture	121	Agricultural land
HA-2	Highwater free builtup area	114	Paved / Builtup area
HB-1	Highwater free natural forest	1244	Natural forest
HB-2	Highwater free shrubs	1233	Shrubs
HB-3	Highwater free production forest	1242	Production forest
HG-1	Highwater free natural grassland	1202	Natural meadows
HG-1-2	Highwater free grassland (natural or production)	1202	Production / natural meadows
HG-2	Highwater free production grassland	1201	Production meadows
HM-1	Highwater free reeds	1807	Reeds and other helophytes
HR-1	Highwater free herbaceous vegetation	1212	Herbaceous vegetation
H-REST	Highwater free temporarily bare	1250	Rest
I.1	Dynamic sweet to brackish shallow water	106	Shallow water
I.3	Slightly dynamic sweet to brackish shallow water	106	Shallow water
II.1	Gravel bars	111	Bare river bar
II.2	Sweet sand bars	111	Bare river bar
II.2-3	Sweet sand bars/ sweet mud banks	111	Bare river bar
II.3	Sweet mud banks	111	Bare river bar
II.4-5	Mid to highly dynamic brackish and salty bars	111	Bare river bar
III.2	Highly dynamic hard substrate influenced by sweet to brackish water	113	Paved / Builtup area
III.2-3	Low dynamic hard substrate influenced by sweet to brackish water	113	Paved / Builtup area
III.4	Low dynamic hard substrate influenced by brackish water	113	Paved / Builtup area
III.8	Low dynamic hard substrate on the outside berm influenced by salty water	113	Paved / Builtup area
IV.1	Species poor helophytes in shallow sweet water	1807	Reeds and other helophytes
IV.3-IV.8	Species poor helophytes swamp	1224	Bulrush / other helophytes
IV.7	Brackish helophyte culture	1807	Reeds and other helophytes
IV.8-9	Species poor helophytes swamp/Species rich reed swamp	1807	Reeds and other helophytes
IX.a	Agriculture on the shoreline	121	Agricultural land
OK-1	Unvegetated natural levee	1250	Bare levee
O-UA-1	Natural levee or floodplain agriculture	121	Agricultural land
O-UA-2	Natural levee or floodplain builtup area	114	Paved / Builtup area
O-UB-1	Natural levee or floodplain forest	1245	Natural forest
O-UB-2	Natural levee or floodplain shrubs	1231	Shrubs
O-UB-3	Natural levee or floodplain production forest	1242	Production forest
O-UG-1	Natural levee or floodplain grass land	1202	Natural grassland
O-UG-1-2	Natural levee or floodplain grass land (natural or production)	1202	Production / natural meadows
O-UG-2	Natural levee or floodplain production grassland	1201	Production meadows
O-UK-1	Natural levee or floodplain unvegetated	1250	Bare levee
O-UR-1	Natural levee or floodplain herbaceous vegetation	1212	Herbaceous vegetation
O-U-REST	Natural levee or floodplain temporarily bare	1250	Rest
R	Temporarily bare	1250	Rest
REST	Temporarily bare	1250	Rest
REST-O	Temporarily bare	1250	Rest
REST-O-T	Temporarily bare	1250	Rest
REST-T	Temporarily bare high water free	1250	Rest
RnM	Moderately deep side channel	105	Side channel
RnMz-h	Moderately deep side channel	105	Side channel
RnOz-h	Moderately deep side channel	105	Side channel
RvD	(Very) deep	106	River accompanying water
RvDz-k-h	(Very) deep	106	River accompanying water
RvDz-k-h/RvMz-k-h	(Very) deep / moderately deep	106	River accompanying water
RvM	Moderately deep water	106	River accompanying water
RvMz-k-h	Moderately deep water	106	River accompanying water
RvO	Shallow water	106	River accompanying water
RvOz-k-h	Shallow water	106	River accompanying water
RwD	(Very) deep water	106	River accompanying water
RwM	Moderately deep water	106	River accompanying water
RwMz-h	Moderately deep water	106	River accompanying water
RwO	Shallow water	106	River accompanying water

Ecotope code	Description	Roughness code baseline 4	Roughness code description
RwOz-h	Shallow water	106	River accompanying water
RzD	Deep main channel	102	Main channel
RzDz-h	Deep main channel	102	Main channel
RzM	Moderately deep main channel	102	Main channel
RzMz-h	Moderately deep main channel	102	Main channel
RzO	Shallow main channel	102	Main channel
RzOz-h	Shallow main channel	102	Main channel
UA-1	Floodplain agriculture	121	Agricultural land
UA-2	Floodplain builtup area	114	Paved / Builtup area
UB-1	Floodplain forest	1245	Natural forest
UB-2	Floodplain shrubs	1231	Shrubs
UB-3	Floodplain production forest	1242	Production forest
UG-1	Floodplain grass land	1202	Natural grassland
UG-1-2	Floodplain grass land (natural or production)	1202	Production / natural meadows
UG-2	Floodplain production grass land	1201	Production meadows
UG-HA-2	Floodplain production grass land / Highwater free production grass land	114	Production meadow / builtup
U-HG-2	Floodplain production grass land / Highwater free builtup area	1201	Production meadow
UM-1	Natural levee or floodplain reed	1807	Reeds and other helophytes
UR-1	Floodplain herbaceous vegetation	1212	Herbaceous vegetation
U-REST	Floodplain temporarily bare	1250	Rest
V.1-2	Floodplain swamp	1804	Herbaceous vegetation
V.2	Species poor reed swamp	1804	Reeds and other helophytes
V.2/UR-1-2	Species poor reed swamp/floodplain natural grass land/floodplain production grass land	1202	Herbaceous vegetation
V.4/UR-1	Species poor, stucture rich floodplain herbaceous vegetation	1212	Herbaceous vegetation
VI.2	Softwood shrubs	1231	Shrubs
VI.2-3	Softwood shrubs or pioneer softwood forest	1231	Shrubs
VI.4	Softwood forest	1245	Natural forest
VI.5	Floodplain forest	1242	Natural forest
VI.7	Floodplain willow production forest	1232	Willow production forest
VI.8	Production forest on shoreline	1242	Production forest
VI.g	Production / natural grass land	1202	Production / natural meadows
VI.nb	Natural forest	1245	Natural forest
VI.pb	Production forest	1242	Production forest
VII.1	Swampy inundation grass land	1202	Natural grassland
VII.1-2	Swampy inundation grass land / structure rich grass land	1202	Natural grassland
VII.1-2-3	Swampy inundation grass land / structure rich grass land/ production grass land	1202	Production / natural meadows
VII.1-3	Swampy inundation grass land / structure rich grass land/ production grass land	1202	Production / natural meadows
VII.2	Structure rich grass land	1202	Natural meadows
VII.3	Production grass land	1201	Production meadow

Appendix B Adapted roughness characterization file for vegetation roughness

codes 100-300 Unvegetated floodplain land cover
codes 1200-1400: Emergent and submerged vegetation and
codes 1800-1900: Combinations of ecotopes

```
# CODE 101-300   : Ruwheids formulering volgens de formule van White-Colebrook
# r_code       : de ruwheids code
# a          : k-Nikuradse (normaal of eb)        (0.0001 - 0.20 - 100.)
# b          : k-Nikuradse (vloed)              (0.0001 - 0.20 - 100.)
# c          : geen betekenis
# d          : geen betekenis
#
r_code =  101  a =  0.20            # default waarde
r_code =  102  a =  0.15            # diepe bedding
r_code =  103  a =  0.15            # ondiepe bedding
r_code =  104  a =  0.15            # strang
r_code =  105  a =  0.20            # nevengeul
r_code =  106  a =  0.05            # plas/haven/slikkige oever
r_code =  111  a =  0.15            # kribvakstrand/zandplaat/grindplaat
r_code =  112  a =  0.40            # ruwe oever
r_code =  113  a =  0.30            # steenbekleding
r_code =  114  a =  0.60            # bebouwd/verhard terrein
r_code =  115  a =  1.00            # bebouwd terrein
r_code =  116  a =  0.20            # verhard terrein
r_code =  121  a =  0.20            # akker
r_code =  122  a =  0.25            # strooisel
r_code =  131  a =  0.63            # vaste laag Nijmegen
r_code =  132  a =  0.34            # vaste laag St. Andries
r_code =  133  a =  0.68            # bodem kribben Erlecom
r_code =  141  a =  0.10            # ketelmeer oost
r_code =  142  a =  0.10            # ketelmeer west
r_code =  143  a =  0.10            # vossemeer
# Additional codes (structuuraanpassing)
r_code =  200  a =  0.09            # kribvakstrand/zandplaat/grindplaat
r_code =  201  a =  0.12            # kribvakstrand/zandplaat/grindplaat
r_code =  202  a =  0.195            # kribvakstrand/zandplaat/grindplaat
r_code =  203  a =  0.24            # kribvakstrand/zandplaat/grindplaat
r_code =  204  a =  0.24            # ruwe oever
r_code =  205  a =  0.32            # ruwe oever
r_code =  206  a =  0.52            # ruwe oever
r_code =  207  a =  0.64            # ruwe oever
r_code =  208  a =  0.18            # steenbekleding
r_code =  209  a =  0.24            # steenbekleding
r_code =  210  a =  0.39            # steenbekleding
r_code =  211  a =  0.48            # steenbekleding
r_code =  212  a =  0.36            # bebouwd/verhard terrein
r_code =  213  a =  0.48            # bebouwd/verhard terrein
r_code =  214  a =  0.78            # bebouwd/verhard terrein
r_code =  215  a =  0.96            # bebouwd/verhard terrein
r_code =  216  a =  0.60            # bebouwd terrein
r_code =  217  a =  0.80            # bebouwd terrein
r_code =  218  a =  1.30            # bebouwd terrein
r_code =  219  a =  1.60            # bebouwd terrein
r_code =  220  a =  0.12            # verhard terrein
r_code =  221  a =  0.16            # verhard terrein
r_code =  222  a =  0.26            # verhard terrein
r_code =  223  a =  0.32            # verhard terrein
r_code =  224  a =  0.12            # akker
r_code =  225  a =  0.16            # akker
r_code =  226  a =  0.26            # akker
r_code =  227  a =  0.32            # akker
r_code =  228  a =  0.15            # strooisel
r_code =  229  a =  0.20            # strooisel
r_code =  230  a =  0.325            # strooisel
r_code =  231  a =  0.40            # strooisel
# CODE 1201-1400 : Ruwheids formulering voor door- en overstroomde vegetatie
```

```
# r_code : de ruwheids code
# a : de vegetatie hoogte (0.001 - 0.2 - 50.)
# b : de vegetatie dichtheid (0.0001 - 0.2 - 100.)
# c : drag coefficient (0.1 - 1.8 - 10.)
# d : k-Nikuradse (onderlaag begroeiing) (0.001 - 0.2 - 100.)
#
r_code = 1201 a = 0.06 b = 45. c = 1.8 d = 0.1 # productiegrasland
r_code = 1202 a = 0.10 b = 12. c = 1.8 d = 0.1 # natuuurlijk gras/hooiland
r_code = 1203 a = 0.20 b = 15. c = 1.8 d = 0.1 # verruigd grasland
r_code = 1211 a = 0.30 b = 3. c = 1.8 d = 0.1 # akkerdistelruigte
r_code = 1212 a = 0.56 b = 0.23 c = 1.8 d = 0.1 # droge ruigte
r_code = 1213 a = 0.50 b = 0.56 c = 1.8 d = 0.1 # dauwbraamruigte
r_code = 1214 a = 0.95 b = 0.13 c = 1.8 d = 0.1 # wilgenroosje ruigte
r_code = 1215 a = 2.00 b = 0.16 c = 1.8 d = 0.1 # rietruigte
r_code = 1221 a = 0.35 b = 0.25 c = 1.8 d = 0.1 # natte ruigte homogeen
r_code = 1222 a = 0.30 b = 1.2 c = 1.8 d = 0.1 # zegge homogeen
r_code = 1223 a = 1.00 b = 0.4 c = 1.8 d = 0.1 # rietgras homogeen
r_code = 1224 a = 0.50 b = 1.2 c = 1.8 d = 0.1 # biezen homogeen
r_code = 1225 a = 1.50 b = 0.35 c = 1.8 d = 0.1 # lisdodde homogeen
r_code = 1226 a = 2.50 b = 0.37 c = 1.8 d = 0.1 # riet homogeen
r_code = 1231 a = 6.00 b = 0.13 c = 1.5 d = 0.4 # zachthoutstruweel
r_code = 1232 a = 3.00 b = 0.041 c = 1.5 d = 0.4 # griend
r_code = 1233 a = 5.00 b = 0.17 c = 1.5 d = 0.4 # doornstruweel
r_code = 1241 a = 10.00 b = 0.011 c = 1.5 d = 0.3 # productiebos hardhout
r_code = 1242 a = 10.00 b = 0.010 c = 1.5 d = 0.3 # productiebos zachthout
r_code = 1243 a = 10.00 b = 0.016 c = 1.5 d = 0.3 # productiebos naaldhout
r_code = 1244 a = 10.00 b = 0.023 c = 1.5 d = 0.4 # hardhoutooibos
r_code = 1245 a = 10.00 b = 0.028 c = 1.5 d = 0.6 # zachthoutooibos
r_code = 1246 a = 3.00 b = 0.024 c = 1.5 d = 0.2 # boomgaard laagstam
r_code = 1247 a = 6.00 b = 0.01 c = 1.5 d = 0.2 # boomgaard hoogstam
r_code = 1250 a = 0.15 b = 0.15 c = 1.8 d = 0.1 # pioniervegetatie
#
# new codes FC2015 structuuraanpassing
r_code = 1249 a = 0.11 b = 24.5 c = 1.8 d = 0.1 # Production meadow
r_code = 1251 a = 0.03 b = 19.727 c = 1.8 d = 0.1 # Production meadow
r_code = 1252 a = 0.06 b = 9.591 c = 1.8 d = 0.1 # Production meadow
r_code = 1253 a = 0.03 b = 12.909 c = 1.8 d = 0.1 # Production meadow
r_code = 1254 a = 0.95 b = 0.199 c = 1.8 d = 0.1 # Natural grass and hayland
r_code = 1255 a = 0.43 b = 0.158 c = 1.8 d = 0.1 # Natural grass and hayland
r_code = 1256 a = 0.6 b = 0.035 c = 1.8 d = 0.1 # Natural grass and hayland
r_code = 1257 a = 0.35 b = 0.035 c = 1.8 d = 0.1 # Natural grass and hayland
r_code = 1258 a = 0.89 b = 0.067 c = 1.8 d = 0.1 # Dry herbaceous vegetation
r_code = 1259 a = 0.59 b = 0.128 c = 1.8 d = 0.1 # Dry herbaceous vegetation
r_code = 1260 a = 0.81 b = 0.034 c = 1.8 d = 0.1 # Dry herbaceous vegetation
r_code = 1261 a = 0.44 b = 0.021 c = 1.8 d = 0.1 # Dry herbaceous vegetation
r_code = 1262 a = 2 b = 0.8 c = 1.8 d = 0.1 # Reed-grass
r_code = 1263 a = 0.5 b = 0.8 c = 1.8 d = 0.1 # Reed-grass
r_code = 1264 a = 2 b = 0.2 c = 1.8 d = 0.1 # Reed-grass
r_code = 1265 a = 0.5 b = 0.2 c = 1.8 d = 0.1 # Reed-grass
r_code = 1266 a = 3.5 b = 0.74 c = 1.8 d = 0.1 # Reed
r_code = 1267 a = 1.25 b = 0.74 c = 1.8 d = 0.1 # Reed
r_code = 1268 a = 3.5 b = 0.185 c = 1.8 d = 0.1 # Reed
r_code = 1269 a = 1.25 b = 0.185 c = 1.8 d = 0.1 # Reed
r_code = 1270 a = 4.59 b = 0.177 c = 1.5 d = 0.4 # Softwood shrubs
r_code = 1271 a = 2.7 b = 0.318 c = 1.5 d = 0.4 # Softwood shrubs
r_code = 1272 a = 9.08 b = 0.066 c = 1.5 d = 0.4 # Softwood shrubs
r_code = 1273 a = 5.33 b = 0.042 c = 1.5 d = 0.4 # Softwood shrubs
r_code = 1274 a = 6 b = 0.082 c = 1.5 d = 0.4 # Willow plantation
r_code = 1275 a = 1.5 b = 0.082 c = 1.5 d = 0.4 # Willow plantation
r_code = 1276 a = 6 b = 0.021 c = 1.5 d = 0.4 # Willow plantation
r_code = 1277 a = 1.5 b = 0.021 c = 1.5 d = 0.4 # Willow plantation
r_code = 1278 a = 10 b = 0.34 c = 1.5 d = 0.4 # Thorny shrubs
r_code = 1279 a = 2.5 b = 0.34 c = 1.5 d = 0.4 # Thorny shrubs
r_code = 1280 a = 10 b = 0.085 c = 1.5 d = 0.4 # Thorny shrubs
r_code = 1281 a = 2.5 b = 0.085 c = 1.5 d = 0.4 # Thorny shrubs
r_code = 1282 a = 10 b = 0.112 c = 1.5 d = 0.3 # Softwood production forest
r_code = 1283 a = 10 b = 0.056 c = 1.5 d = 0.3 # Softwood production forest
r_code = 1284 a = 10 b = 0.014 c = 1.5 d = 0.3 # Softwood production forest
r_code = 1285 a = 10 b = 0.007 c = 1.5 d = 0.3 # Softwood production forest
r_code = 1286 a = 10 b = 0.098 c = 1.5 d = 0.4 # Hardwood forest
r_code = 1287 a = 10 b = 0.04 c = 1.5 d = 0.4 # Hardwood forest
```

```
r_code = 1288 a = 10 b = 0.026 c = 1.5 d = 0.4 # Hardwood forest
r_code = 1289 a = 10 b = 0.011 c = 1.5 d = 0.4 # Hardwood forest
r_code = 1290 a = 10 b = 0.155 c = 1.5 d = 0.6 # Softwood forest
r_code = 1291 a = 10 b = 0.067 c = 1.5 d = 0.6 # Softwood forest
r_code = 1292 a = 10 b = 0.036 c = 1.5 d = 0.6 # Softwood forest
r_code = 1293 a = 10 b = 0.018 c = 1.5 d = 0.6 # Softwood forest
r_code = 1294 a = 0.14 b = 0.3 c = 1.8 d = 0.1 # Pioneer vegetation
r_code = 1295 a = 0.07 b = 0.3 c = 1.8 d = 0.1 # Pioneer vegetation
r_code = 1296 a = 0.04 b = 0.075 c = 1.8 d = 0.1 # Pioneer vegetation
r_code = 1297 a = 0.01 b = 0.075 c = 1.8 d = 0.1 # Pioneer vegetation
#
#================================================================================
#
# CODE 1801-1900 : Ruwheids combinatie voor r_codes van 101-600 en 1201-1300
# r_code : de ruwheids code
# a : de r_code van de eerste ruwheid (1 - 1221 - 1300)
# b : de r_code van de tweede ruwheid (1 - 106 - 1900)
# c : het percentage van de eerste r_code (0.001 - 0.75 - 0.999)
# d : het percentage van de tweede r_code (0.001 - 0.25 - 0.999)
#
r_code = 1801 a = 1221 b = 106 c = 0.75 d = 0.25 # natte ruigte met 25% water
r_code = 1802 a = 1245 b = 1801 c = 0.05 d = 0.95 # 5% zachthoutooibos en 95%
 # natte ruigte met 25% water
r_code = 1803 a = 1222 b = 122 c = 0.75 d = 0.25 # zegge met 25% strooisel
r_code = 1804 a = 1223 b = 106 c = 0.75 d = 0.25 # rietgras met 25% water
r_code = 1805 a = 1224 b = 106 c = 0.75 d = 0.25 # biezen met 25% water
r_code = 1806 a = 1225 b = 106 c = 0.75 d = 0.25 # lisdodde met 25% water
r_code = 1807 a = 1226 b = 122 c = 0.75 d = 0.25 # riet met 25% strooisel
#
# combinaties uit de vegetatie opname van DON 2004
r_code = 1811 a = 1250 b = 1245 c = 0.95 d = 0.05 # pioniervegetatie met
 # 5% zachthoutooibos
r_code = 1812 a = 1202 b = 1245 c = 0.80 d = 0.20 # natuurlijkgrasland met
 # 20% zachthoutooibos
r_code = 1813 a = 1203 b = 1231 c = 0.80 d = 0.20 # verruigdgrasland met
 # 20% zachthoutstruweel
r_code = 1814 a = 1223 b = 1231 c = 0.95 d = 0.05 # rietgras homogeen met
 # 5% zachthoutstruweel
r_code = 1815 a = 1226 b = 1231 c = 0.70 d = 0.30 # riet homogeen met
 # 30% zachthoutstruweel
r_code = 1816 a = 1231 b = 1245 c = 0.80 d = 0.20 # zachthoutstruweel met
 # 20% zachthoutooibos
r_code = 1817 a = 1221 b = 1245 c = 0.95 d = 0.05 # natte ruigte homogeen met
 # 5% zachthoutooibos
r_code = 1818 a = 1221 b = 1231 c = 0.70 d = 0.30 # natte ruigte homogeen met
 # 30% zachthoutstruweel
r_code = 1819 a = 1212 b = 1231 c = 0.90 d = 0.10 # droge ruigte met
 # 10% zachthoutstruweel
#
# combinaties FC2015 (structuuraanpassing) codes 1804 en 1807
r_code = 1820 a = 1262 b = 106 c = 0.75 d = 0.25 # rietgras met 25% water
r_code = 1821 a = 1263 b = 106 c = 0.75 d = 0.25 # rietgras met 25% water
r_code = 1822 a = 1264 b = 106 c = 0.75 d = 0.25 # rietgras met 25% water
r_code = 1823 a = 1265 b = 106 c = 0.75 d = 0.25 # rietgras met 25% water
r_code = 1830 a = 1266 b = 122 c = 0.75 d = 0.25 # riet met 25% strooisel
r_code = 1831 a = 1267 b = 122 c = 0.75 d = 0.25 # riet met 25% strooisel
r_code = 1832 a = 1268 b = 122 c = 0.75 d = 0.25 # riet met 25% strooisel
r_code = 1833 a = 1269 b = 122 c = 0.75 d = 0.25 # riet met 25% strooisel
```